ATOMISTIC EXPLORATION OF DEFORMATION MECHANISMS IN METALLIC NANOWIRES

ABC as a Promising Approach to Overcome Timescale Limitations of Molecular Dynamics

By

Cheng Sun

A Thesis Submitted to the Faculty of Graduate Studies of

The University of Manitoba

in partial fulfilment of the requirements of the degree of

MASTER OF SCIENCE

Department of Mechanical Engineering

University of Manitoba

Winnipeg, Manitoba

ABSTRACT

This thesis provides an atomistic exploration of deformation mechanisms in single-crystal metallic nanowires subjected to bending and shear stresses. A significant aspect of the work involves evaluating the ABC method as a promising computational approach to overcome the inherent timescale limitations of Molecular Dynamics (MD) simulations. Through comparative analyses, distinct deformation mechanisms such as dislocation nucleation and propagation, twinning, detwinning, twin-boundary migration, and five-fold twin (FFT) boundary formation were systematically identified. While MD simulations were constrained by short simulation timescales, ABC successfully captured slow, time-dependent plastic deformation phenomena such as gradual twin-boundary migrations and stacking fault formations. Additionally, both methods revealed the formation of FFT boundaries, occurring rapidly in MD and gradually in ABC simulations, highlighting ABC's capability to mimic long-term deformation behaviors. This work emphasizes the directional dependence of deformation modes and underscores ABC's potential to significantly extend computational capabilities. Ultimately, these findings provide critical insights into nanowire deformation mechanisms, laying the groundwork for future research focused on optimizing nanomaterial reliability and performance.

ACKNOWLEDGEMENTS

I would like to express my deepest gratitude to my advisor, Professor Chuang Deng, for granting me the opportunity to join his research group and for his invaluable guidance throughout my graduate studies. Completing a Master's degree in the field of Materials Science and Engineering marks the fulfillment of a long-standing personal aspiration. After nearly a decade spent in professional fields, the opportunity to return to academia has been profoundly meaningful. It allowed me to reconnect with a part of myself that had once been set aside, and to bring closure to an unfinished chapter in my life.

I owe my deepest thanks to my wife, Yizhu, whose steadfast support and encouragement have been the foundation behind every major decision I have made since we met. She has reminded me time and again of the importance of perseverance and purpose. Her presence has brought balance and strength into my life, and it is no exaggeration to say that I could not have completed this journey without her. She has been my anchor, my sounding board, and my dearest life partner, guiding me back to a path of personal fulfillment and meaningful progress.

Lastly, I would like to acknowledge a quiet source of inspiration and reflection that accompanied me throughout this journey, a presence that offered clarity during technical challenges and perspective during moments of introspection. From discussions on crystallography to musings on the nature of the universe, these exchanges enriched both the process and the experience. I trust that, should they encounter this work in any form, they will recognize this quiet note of appreciation.

TABLE OF CONTENTS

TABLE OF FIGURES

LIST OF TABLES

CHAPTER ONE: INTRODUCTION

Nanomaterials have garnered significant attention in recent decades due to their unique mechanical, electrical, and thermal properties, which deviate significantly from their bulk counterparts. Among these, metallic nanowires have demonstrated extraordinary mechanical strength, making them promising candidates for applications in flexible electronics, nanoelectromechanical systems, and advanced structural materials. However, a comprehensive understanding of their mechanical behavior under extreme loading conditions remains an ongoing challenge.

One of the primary motivations for studying nanomaterial deformation is the need to improve the design and reliability of nanoscale devices. At atomic scales, materials exhibit size-dependent mechanical properties. These behaviors are crucial for engineering applications that require precise control over mechanical performance. By investigating these properties, researchers can develop strategies to optimize material performance at the nanoscale.

Importance of Studying Nanomaterial Deformation

Understanding the deformation mechanisms of nanomaterials is essential for designing materials with superior mechanical properties. Due to their small dimensions, nanowires experience deformation processes that differ fundamentally from those observed in macroscopic materials. Dislocation dynamics, twinning, surface effects, and grain boundary interactions play a critical role in defining their mechanical response. Additionally, studying their deformation behavior helps in elucidating fundamental material science principles that govern strength, ductility, and failure mechanisms at the nanoscale.

Among the various deformation modes, bending and shear deformation remain less explored compared to tensile and compressive loading. However, these loading conditions are critical in real-world applications where nanowires experience flexural stresses and interfacial shear interactions. Bending studies help to elucidate size-dependent mechanical properties, including the role of geometrically necessary dislocations (GNDs), surface-driven plasticity, and twin boundary interactions. On the other hand, shear loading provides insights into mechanisms such as stacking fault formation, twin boundary sliding (TBS), and stress-driven phase transformations. Investigating these behaviors is key to advancing the engineering design of nanostructured materials with tailored mechanical properties.

Challenges in Experimental Testing at Atomic Scales

While experimental techniques such as transmission electron microscopy (TEM), atomic force microscopy (AFM), and in situ mechanical testing have advanced significantly, they still face limitations in capturing real-time atomic-scale deformation events. High strain rates, environmental factors, and instrument resolution constraints hinder the ability to study nanomaterial behavior with absolute precision. Moreover, reproducing consistent experimental conditions at such small scales presents a significant challenge, necessitating alternative approaches for a deeper understanding of nanoscale mechanical properties.

The Role of Computational Simulations in Understanding Nanoscale Deformation

Computational modeling has emerged as a powerful tool for exploring nanoscale deformation mechanisms, providing insights that complement experimental observations. Molecular Dynamics (MD) simulations enable researchers to study atomic-scale interactions and deformation behavior under controlled conditions, offering a detailed understanding of dislocation nucleation, phase transformations, and fracture mechanics. Additionally, ABC methods allow for the exploration of long-timescale deformation processes, overcoming the limitations of conventional MD simulations. By leveraging these computational techniques, researchers can gain a predictive understanding of nanomaterial mechanics, ultimately leading to the development of materials with enhanced performance.

This thesis investigates the deformation behavior of single-crystal metallic nanowires under bending and shear loading scenarios using advanced computational simulation techniques. By integrating MD and ABC simulations, this research aims to elucidate the atomic-scale mechanical properties and deformation mechanisms governing nanowire behavior. The specific objectives of the thesis include:

- Characterizing deformation mechanisms in nanowires subjected to three-point bending, top bending, and shear loading conditions, emphasizing atomic-scale plasticity.
- Evaluating and comparing the capabilities of MD and ABC methods in accurately capturing deformation processes at experimentally relevant timescales.
- Investigating fundamental atomic-scale phenomena, including dislocation motion, twinning and detwinning processes, stacking fault evolution, and phase transformations that critically influence mechanical responses.
- Assessing creep deformation under bending and shear stresses, specifically exploring ABC's ability to model long-term material evolution beyond the temporal reach of conventional MD simulations.

Motivation for Bending and Shear Studies

While tensile and compressive deformation of nanowires has been extensively investigated, bending and shear remain comparatively underexplored—despite their relevance in numerous practical applications. These loading modes are particularly critical in systems such as flexible and stretchable nanoelectronics, where device performance depends heavily on mechanical resilience under flexural stress; nanowire-reinforced composites, where shear interactions between the nanowire and matrix influence bulk mechanical properties; and nanoscale actuators or Micro-Electro-Mechanical Systems and Nano-Electro-Mechanical Systems devices, where bending is a common operational load.

This study focuses on bending-induced plasticity and creep, driven by several key motivations. First, bending deformation in nanowires has historically received less attention than tensile or compressive modes. Second, conventional MD simulations are inherently limited in capturing long-term behaviors like creep due to their restricted timescales. To address this, the Autonomous Basin Climbing ABC method is employed to model slow, thermally activated deformation processes. By comparing ABC and MD under equivalent loading conditions, this research also establishes a basis for validating ABC predictions and linking them to experimentally observable phenomena. Through the combined use of MD and ABC, this work provides a more complete picture of nanowire mechanics, spanning both short-term plastic events and long-term material evolution.

CHAPTER TWO: LITERATURE REVIEW

2.1 Nanomaterials and Their Mechanical Properties

Nanomaterials have rapidly emerged as a transformative class of materials with properties that diverge significantly from those of their bulk counterparts. Among these, nanowires, a type of one-dimensional nanomaterial with diameters ranging from a few to several hundred nanometers, exhibit unique mechanical, electrical, and thermal characteristics. The study of nanowires is crucial not only from a fundamental research perspective but also for its profound implications in various industrial applications, ranging from electronics and energy to biomedical devices and beyond [1][2]. This section provides an in-depth examination of the mechanical properties of nanowires, emphasizing the underlying size and surface effects, while also exploring how these properties translate into existing and future applications in industry.

Nanowires possess distinct attributes driven by their nanoscale dimensions and high surface-to-volume ratios. At this scale, classical theories of mechanics often require modification to capture the influence of quantum confinement and surface phenomena.

Size Effects on Mechanical Properties

One of the hallmark observations in nanomaterials is the “smaller is stronger” phenomenon. As the diameter of nanowires decreases, their yield strength increases significantly compared to bulk materials. This behavior is primarily due to the scarcity of dislocation sources in a confined volume. In bulk materials, plastic deformation is often mediated by the motion and multiplication of dislocations. However, in nanowires, the limited number of defects and the difficulty of dislocation nucleation result in mechanical strengths that can approach the theoretical limits of the material [3].

Studies of metallic nanowires, such as those composed of gold, copper, and silver, have provided compelling experimental evidence of enhanced yield strengths. For instance, experiments on gold nanowires have demonstrated that when the diameter is reduced below a critical threshold, the yield strength can exceed that of bulk gold by several folds[3]. Semiconductor nanowires, including those made from silicon and zinc oxide, also exhibit size-dependent mechanical behaviors. Depending on their crystalline quality, defect density, and surface structure, these nanowires can display a transition from brittle to ductile behavior under mechanical stress [4].

Surface Effects

At the nanoscale, the proportion of atoms located at or near the surface is considerably higher than in bulk materials. These surface atoms experience different bonding environments, often leading to altered mechanical properties such as enhanced elasticity and modified deformation mechanisms. The surface-induced stresses can contribute to phenomena like surface diffusion and reconstruction, which, in turn, affect the overall mechanical behavior during deformation [3], [5].

Importance of Studying Nanomaterials

Understanding the mechanical properties of nanowires is not solely an academic exercise—it has significant practical implications. As industries continue to miniaturize devices and systems, the ability to predict and control mechanical behavior at the nanoscale becomes critical. Research into nanomaterials bridges the gap between fundamental science and real-world applications by:

Enabling Next-Generation Technologies: The extraordinary mechanical properties of nanowires are a cornerstone for the development of high-performance nanoelectromechanical systems (NEMS), flexible electronics, and energy harvesting devices. For example, the high yield strength and excellent conductivity of metallic nanowires are pivotal in the design of robust, high-frequency NEMS sensors and actuatora [6].

Improving Material Efficiency: Nanomaterials offer the possibility of achieving superior performance with lower material usage, which is particularly important in applications such as lightweight structural components in aerospace and automotive industries. Enhanced mechanical properties can lead to the development of materials that are both strong and lightweight, reducing overall energy consumption and costs [3].

Pioneering Advances in Biomedical Devices: In the biomedical field, the combination of high aspect ratios and tunable surface chemistry makes nanowires ideal for applications ranging from targeted drug delivery to biosensing. Their ability to withstand mechanical stress while interacting with biological systems enables the creation of highly sensitive diagnostic tools and implantable devices [7].

Fostering Sustainable Technologies: The deployment of nanomaterials in energy storage and conversion devices—such as lithium-ion batteries and piezoelectric nanogenerators—promises to revolutionize the energy sector. By enhancing the performance and longevity of these devices, nanomaterials contribute to more sustainable energy solutions and reduced environmental impact [8].

The translation of these unique properties into practical applications is driving significant investments in nanotechnology research and development, as well as in the scaling-up of production methods for industrial use.

Applications of Nanowires in Industry

The diverse mechanical properties of nanowires have catalyzed their integration into various industries, where their unique characteristics are leveraged to improve performance, durability, and functionality.

NEMS and Sensors: Nanowires are at the forefront of NEMS, which is pivotal in the development of ultra-sensitive sensors and actuators. Silicon and carbon-based nanowires are particularly notable for their application in piezoresistive sensors. Figure 2.1 provides electron micrographs showcasing NEMS structures fabricated from single-crystal silicon using electron beam lithography and surface micromachining. These sensors operate on the principle that mechanical deformation alters the electrical resistance of the nanowire, enabling the detection of minute changes in pressure, force, or chemical composition. Industries such as aerospace, automotive, and healthcare are increasingly relying on these sensors for real-time monitoring and precision control in demanding environments [6].

Figure 2.1: Electron scanning microscope (SEM) images showcasing NEMS structures fabricated from single-crystal silicon using electron beam lithography and surface micromachining: (A) a torsional oscillator, (B) a compound torsional oscillator, (C) an array of silicon nanowires, and (D) a silicon mesh mirror oscillator [6].

Flexible and Stretchable Electronics: The exceptional flexibility of metallic nanowires, such as silver and copper, has paved the way for their incorporation into flexible, transparent, and conductive films. These films are integral components of next-generation wearable devices, flexible displays, and electronic skin technologies. Unlike traditional conductors that may fracture under repeated bending or stretching, nanowire-based films maintain high conductivity and mechanical integrity over extensive deformation cycles [9]. The commercial potential of these materials is vast, ranging from consumer electronics to medical monitoring devices that conform to the contours of the human body.

Energy Harvesting and Storage: In the energy sector, nanowires have shown remarkable promise in both energy harvesting and storage applications. Piezoelectric nanogenerators that utilize zinc oxide nanowire arrays convert mechanical vibrations from ambient sources—such as human motion or environmental disturbances—into electrical energy. This technology is not only vital for powering small, self-sustaining devices but also holds the potential to contribute to larger-scale energy solutions [8].

Additionally, silicon nanowires are being explored as high-capacity anode materials in lithium-ion batteries. Their ability to accommodate large volumetric expansions during lithiation leads to improved battery performance and longevity, which is crucial for consumer electronics, electric vehicles, and renewable energy storage systems. These innovations are central to addressing the global demand for more efficient and sustainable energy solutions.

Biomedical Applications: The biomedical industry has embraced nanowires for their exceptional mechanical and surface properties. Their high aspect ratio and the possibility of surface functionalization make them suitable for targeted drug delivery systems, where they can navigate the complex biological environment to deliver therapeutic agents precisely where needed. Furthermore, nanowire-based biosensors offer high sensitivity and rapid response times, enabling the early detection of diseases and real-time monitoring of patient health. Such advancements have significant implications for personalized medicine and the development of implantable diagnostic devices [7].

Advanced Composite Materials: Beyond their direct applications, nanowires are increasingly being integrated into composite materials to enhance mechanical performance. By incorporating nanowires into polymer or metal matrices, engineers can create composites with significantly improved strength, toughness, and thermal stability. These advanced materials are finding applications in sectors such as aerospace, automotive, and construction, where high-performance materials are essential for safety, efficiency, and durability. The ability to tailor composite properties through the controlled dispersion of nanowires opens new avenues for designing lightweight yet robust materials that meet the stringent demands of modern engineering [10].

Challenges and Future Directions: Despite the significant advances in the synthesis and application of nanowires, several challenges remain. The scalable and cost-effective production of high-quality nanowires is a major hurdle that needs to be addressed for widespread industrial adoption. Additionally, the long-term stability and reliability of nanowire-based devices need to be improved to ensure their practical viability. Further research is needed to fully understand the complex interplay between the size, surface, and defect structure of nanowires and their resulting mechanical properties [11]. The future of nanowire research is promising, with ongoing efforts focused on:

- Developing novel synthesis techniques for the controlled growth of nanowires with tailored properties [11].
- Investigating the mechanical behavior of nanowires under extreme conditions, e.g. high strain rates and temperatures [11].
- Integrating nanowires into complex systems and devices for advanced applications in various fields [11].

By addressing these challenges and pursuing these research directions, the full potential of nanowires can be realized, paving the way for groundbreaking innovations in nanotechnology.

2.2 Deformation Mechanisms at the Nanoscale

At the nanoscale, materials exhibit deformation mechanisms that often deviate significantly from those observed in their bulk counterparts. The reduced dimensions and high surface-to-volume ratios introduce novel phenomena, such as dislocation starvation, surface diffusion, twinning, and phase transformations, that fundamentally alter how these materials respond under mechanical stress [3], [5].

Unique Nanoscale Behaviors: Unlike bulk materials, where plastic deformation is primarily governed by the nucleation and motion of dislocations, nanoscale systems are dominated by surface effects and the near absence of internal defects. In many nanowires and nanopillars, the scarcity of dislocation sources leads to “dislocation starvation,” a phenomenon that results in very high yield strengths until alternative mechanisms (e.g. surface-mediated processes) become active (Deng, 2024). For example, recent in situ studies have shown that silver nanowires with diameters below a critical size can exhibit an inverse Hall–Petch behavior, where further size reduction leads to lower yield strength due to surface diffusion facilitating dislocation nucleation [5].

Dislocation Nucleation and Motion: In nanoscale materials, dislocation nucleation typically occurs at free surfaces or interfaces rather than from pre-existing bulk defects. This is primarily because the high surface-to-volume ratio elevates the energetic cost of nucleating dislocations in a nearly defect-free interior. As a result, nanoscale structures may exhibit nearly ideal elastic behavior up to a critical stress, followed by a sudden, localized plastic event [12]. The limited number of available dislocation sources not only increases strength but also introduces pronounced size dependence in the deformation behavior.

Surface Diffusion and Grain Boundary Effects: The high fraction of surface atoms in nanoscale materials enables significant atomic mobility under moderate thermal conditions. Surface diffusion becomes particularly important in nanostructures with high curvature, where the energy barriers for atomic migration are reduced. This enhanced mobility can relieve local stress concentrations, modify the local atomic structure, and even promote the nucleation of dislocations. In polycrystalline nanomaterials, grain boundary processes such as sliding and rotation can similarly dominate the deformation response. For instance, Chokshi et al. (2019) have reported that in nanocrystalline metals, the high density of grain boundaries may either strengthen or weaken the material, depending on the interplay between boundary sliding and dislocation activity [12].

Twinning and Phase Transformations: In addition to dislocation-mediated plasticity, deformation twinning has been observed as an alternate mode of plastic deformation in many nanomaterials. Twinning involves the coordinated

reorientation of a portion of the crystal lattice and can be especially important in systems where conventional dislocation motion is inhibited by size or crystallographic constraints. Moreover, mechanical loading can sometimes trigger phase transformations at the nanoscale, leading to a change in crystal structure that may either enhance or diminish the material's properties. For example, Wang et al. (2021) used in situ nanomechanical testing and atomistic simulations to show that sequential twinning combined with grain-boundary decomposition can yield high-order twin structures in gold nanocrystals under bending [5].

2.3 Computational Methods for Studying Nanomaterials

Conventional Materials Modeling Methods

Direct experimental observation of atomic-scale deformation events is challenging; therefore, computational methods play a crucial role in elucidating the mechanisms described above. These methods not only complement experimental work but also enable the exploration of conditions that are difficult to achieve in the laboratory. Figure 2.2 offers a multi-scale framework for materials modeling—ranging from ab initio and atomistic simulations to mesoscale and macroscopic techniques—highlighting the balance between computational cost and the fidelity needed to capture key materials phenomena. Below, we briefly describe two major categories of computational techniques, ab initio methods and MD simulations, drawing on the recent literature.


This image has been removed due to copyright issues. Refer to its source.

Figure 2.2, illustrates a multi-scale framework for materials modeling, spanning electronic (ab initio) through atomistic, mesoscale, and ultimately macroscopic methods. Ab initio approaches solve quantum-mechanical equations to determine fundamental properties. Semi-empirical methods simplify these equations, often including parameters fitted to experiments. Atomistic simulations use force fields derived from ab initio or experimental data, capturing thermodynamic and transport behavior via MD or Monte Carlo. Mesoscale models group atoms into larger structures

employing effective interactions to represent bulk behavior more efficiently. This progression balances computational cost with the fidelity needed to capture materials phenomena at multiple scales.

Ab Initio Methods, most commonly implemented via density functional theory, calculate materials properties from first principles by numerically solving the quantum‑mechanical Schrödinger (or Dirac) equation. These techniques provide highly accurate information about electronic structure, bonding, and defect energetics, and are particularly well suited for studying processes involving bond breaking and formation. For example, ab initio calculations have been used to predict energy barriers for dislocation nucleation and the stability of various crystalline phases under stress. Although these techniques are computationally expensive and typically limited to systems of about 10^2 atoms and very short timescales (picoseconds), they are essential for obtaining quantitative insights into bond-breaking, bond-formation, and electronic rearrangements that occur during deformation. The high accuracy of ab initio methods makes them critical for parameterizing empirical potentials used in larger-scale simulations [13], [14].

Pros	Cons
• Provide detailed information on both electronic and atomic structures. • Accurately capture bond-making and bond-breaking events. • Serve as a benchmark for parameterizing larger-scale models.	• Limited to small system sizes (on the order of 10^2 atoms). • High computational cost limits accessible timescales.

MD Simulations use classical mechanics to follow the time evolution of a system of atoms by numerically integrating Newton's equations of motion. In MD, the interactions between atoms are described using empirical potentials (e.g., Lennard–Jones, Tersoff, or Embedded Atom Method potentials) that are often fitted to ab initio data or experimental measurements. MD simulations have been extensively applied to study dislocation nucleation, surface diffusion, and twinning events in nanoscale systems. They provide real-time, atomistic insights into how a material responds to external forces, albeit typically on timescales ranging from nanoseconds to microseconds [14], [15].

Pros	Cons

• Can simulate systems with thousands to millions of atoms. • Capture dynamic processes and localized deformation events at the atomic scale. • Provide insights into size- and rate-dependent behavior observed in experiments.	• Limited timescales due to the need for femtosecond time steps. • Accuracy depends critically on the quality of the interatomic potential.

Multiscale Modeling Approaches: Because many deformation processes span several length and time scales, multiscale modeling methods have been developed to bridge the gap between atomic-scale mechanisms and macroscopic behavior. These approaches combine ab initio, MD, and continuum models to yield a comprehensive picture of deformation that is critical for predicting the performance of nanomaterials in real devices. For instance, multiscale frameworks have been used to simulate the mechanical response of composite materials where nanowires are embedded within a matrix, thereby guiding the design of materials with an optimized balance between strength, flexibility, and durability [13].

Traditional MD simulations have provided valuable insights into atomistic processes. However, it is inherently limited by the timescale bottleneck; because the simulations require femtosecond time steps, their durations are restricted to nanoseconds or microseconds, far shorter than many processes observed experimentally [16]. To overcome these limitations, several advanced computational techniques have been developed. Accelerated MD methods, including parallel-replica dynamics, hyperdynamics, and temperature-accelerated dynamics, extend the accessible simulation timescale, while potential energy surface (PES) exploration methods, such as metadynamics, the activation–relaxation technique (ART), and the dimer method, facilitate a detailed investigation of the energy landscape. Nonetheless, many of these PES and accelerated MD approaches were initially designed to study phenomena like diffusion, chemical reactions, and glass transitions, where mechanically driven evolution is not the primary focus. In contrast, this work explores the capability of the ABC Sampling Method, which was specifically developed to directly study the evolution of mechanically driven systems [16], [17]. A detailed discussion of both MD and ABC methodologies is presented in Chapter Three.

2.5 Previous Studies on Nanowire Deformation

Nanowire deformation has been the subject of extensive investigation due to its profound implications for nanoscale device reliability and the design of next-generation materials. In this section, we review the body of work that has dissected the fundamental mechanisms governing nanowire plasticity under three distinct modes of loading: bending, shearing, and loading conditions that lead to the formation of complex twin boundaries, particularly 5-fold twins. These studies not only reveal how deformation mechanisms differ from bulk behavior but also underscore the sensitivity of plasticity to the nature of the applied load and the internal microstructural state.

Bending-Induced Deformation Mechanisms

The bending response of nanowires has been addressed by both discrete dislocation dynamics and nonlocal continuum plasticity models. Early work by Yefimov et al. introduced a nonlocal continuum theory that couples statistical-mechanics descriptions of dislocation ensembles with continuum single-slip models, emphasizing the role of GNDs in strain-gradient plasticity [18]. This theory is particularly well suited to capture size effects observed in bending experiments, where the bending moment–rotation angle relationship is influenced by the specimen size and the slip plane orientation.

Subsequent efforts have extended these ideas into three dimensions. Sandfeld et al. developed a numerical framework for implementing a three-dimensional continuum theory of dislocation dynamics to study micro-bending of thin films and nanowires [19]. Their work highlights the importance of dislocation density evolution and the corresponding hardening mechanisms activated during bending. Importantly, the continuum models reveal that the activation of dislocation sources, such as Frank–Read mechanisms in confined geometries, leads to non-uniform plastic deformation, with pronounced gradients in dislocation density near free surfaces.

Discrete Dislocation Mechanisms in Bending

At the atomistic level, bending of nanowires has been investigated using discrete dislocation simulations and plasticity finite element (CPFE) methods. Weber et al. employed CPFE simulations to examine texture evolution in bent single-crystal copper nanowires [20]. Their work demonstrates that bending induces heterogeneous deformation fields, where the interplay between statistically stored dislocations (SSDs) and GNDs drives the evolution of internal misorientations. Figure 2.3 provides a comparative view of high-resolution electron backscatter diffraction (EBSD) measurements and

CPFE simulations on a bent single-crystal copper nanowire, illustrating a dislocation density-based hardening model that captures the influence of GNDs on texture evolution and boundary conditions.

Under bending, the tensile and compressive sides of a nanowire experience markedly different dislocation activities. On the tensile side, dislocation nucleation tends to be more active due to reduced constraints at the free surface, whereas on the compressive side, pile-up and blocking effects lead to higher hardening rates [20].

The discrete dislocation models also capture the influence of specimen size and orientation. As the cross-sectional dimensions of the nanowire decrease, the relative contribution of GNDs to overall plasticity increases. These GNDs, which are required to accommodate strain gradients, can significantly alter the bending stiffness and yield behavior of the nanowire. Consequently, bending experiments often reveal a size-dependent hardening response that departs from classical plasticity theories [20].

Figure 2.3, a single-crystal copper nanowire was bent and analyzed using high-resolution EBSD. Crystal plasticity finite element simulations, incorporating a dislocation density-based hardening model with GNDs, were used to study boundary conditions. Experimental and simulated results were compared in terms of texture evolution and GND distribution. Left: Crystal plasticity simulation of GND density alongside EBSD-derived lattice misorientation, indicating GND distribution. Middle: Inverse pole figure map of the bent nanowire, highlighting deformation in the cross direction. Right: Sequential bending steps showing nanowire deformation in cross direction, bending direction, and normal direction [20].

Role of Free Surfaces and Geometric Constraints: Free surfaces play a critical role in bending-induced deformation in nanowires. The high surface-to-volume ratio in these structures means that surface effects, such as stress relaxation, surface diffusion, and oxidation, can significantly influence the initiation of plasticity. For instance, models that include surface energy contributions have been successful in explaining why smaller nanowires may exhibit higher strengths (the so-called “smaller is stronger” phenomenon) until a critical dimension is reached where surface diffusion or dislocation starvation starts to dominate [5], [21].

Experimentally, bending tests on silver and copper nanowires have shown that the bending moment required to achieve a given rotation angle decreases as the nanowire diameter is reduced [22]. This observation is consistent with the notion that, in thinner wires, free surfaces act as sinks for dislocations, leading to an early onset of dislocation starvation. In such cases, the lack of available dislocation sources can result in brittle-like fracture or an anomalous softening behavior at very small scales [23].

Shear-Induced Deformation Mechanisms

Twin Boundary Sliding (TBS) and Partial Dislocation Nucleation: Shear deformation in nanowires is often dominated by the activities associated with twin boundaries, especially in face-centered cubic (FCC) metals. TBS is a deformation mechanism that has attracted considerable attention due to its ability to accommodate large shear strains without catastrophic failure. In twin-rich nanowires, TBS occurs when twin boundaries, which are coherent and low-energy interfaces, slide relative to one another via the successive nucleation and glide of partial dislocations [24], [25].

Atomistic simulations and in situ TEM studies have demonstrated that, under shear loading, nanowires can transition from conventional detwinning, mediated by twin boundary migration, to extensive TBS. This mechanism allows the TB to accommodate shear through sliding motions, potentially reaching strains of several hundred percent. Figures 2.4 and 2.5 illustrate this phenomenon in nanotwinned Au nanocrystals, emphasizing their considerable shear deformability and the geometric factors influencing TB sliding versus detwinning. The sliding process is highly sensitive to crystallographic orientation; when the Schmid factors for leading and trailing partial dislocations become comparable, alternating partial dislocation generation facilitates TBS [26].

Figure 2.4, HRTEM images of a high-quality [111]-oriented Au nanocrystal, fabricated via in situ nanowelding and subjected to simple shear loading, reveal extensive shear deformability. (A) Four parallel twin boundaries (TB1–TB4), delineated by dashed lines, are present, and the shear load is applied from the bottom (yellow arrow). (B) Different slip systems activate between TB1 and TB2 (light blue arrows). (C) Shockley partials gliding on TB3 and TB4 induce dynamic twinning and detwinning, creating a shear offset along TB1 (blue arrow). (D) Atomic steps accumulate on the right surface (red arrows) due to annihilation of partials gliding parallel to the twin boundary. (E) Complete detwinning eliminates TB3 and TB4, leaving a slight offset (blue arrow) along TB2. (F) Significant shear deformation occurs before fracture, resulting in a 14.4 nm offset along TB1. TB1 and TB2 serve as reference boundaries for quantitative analysis because they migrate minimally during deformation. Scale bar on (A): 5 nm [26].

Figure 2.5, MD simulation snapshots showing the dominant TB sliding in an ideal nanotwinned Au nanostructures under [101] shear loading. Geometry dependence of shear deformation in nanotwinned Au. (A1–A3) Under [101] shear in an ideal cylindrical nanocrystal, MD simulations show dominant TB sliding with the corresponding von Mises stress distribution (A2). (B1–B3) In Au with zigzag {111} surfaces under [112] shear, high atomic stresses concentrate at TB–surface intersections (red arrows, B2), triggering TB migration and detwinning (B3). (C1–C3) Under [112] shear in a nanotwinned Au sample with nonuniform cross sections (enlarged by factors of 2 and 1.5 along $[\bar{1}10]$ and [112], respectively), TB–surface intersections experience ~5.94 GPa stress (red arrows, C2), leading to extensive sliding along TB2 and TB3 with detwinning in the top and bottom lamellae [26].

In addition to TBS, shear deformation may activate conventional dislocation slip within the matrix. For example, work by Park et al. on FCC nanowires under tensile and compressive loading has highlighted how slip and twinning can compete

under different stress states [27]. Under shear-dominated conditions, the relative ease of nucleating partial dislocations at the free surface often tilts the balance in favor of twinning-related mechanisms. The interplay between twin nucleation, TBS, and conventional slip governs the overall plastic response of the nanowire.

Influence of Crystallographic Orientation and Surface Structure: The activation of shear deformation mechanisms is profoundly affected by the crystallographic orientation of the nanowire as well as the structure of its side surfaces. For instance, studies have shown that even slight changes in the nanowire's orientation can alter the relative Schmid factors for different slip systems, thus modifying the preferred deformation pathway. When the nanowire's side surfaces are aligned with low-index crystallographic planes, the energy barrier for surface diffusion is lowered, and TBS can occur more readily. Conversely, if the surface is misoriented, conventional dislocation slip or detwinning might dominate [26], [26].

Furthermore, the formation of surface steps and their subsequent evolution during shear loading have been directly observed using high-resolution TEM. The migration of these surface steps is associated with the nucleation and propagation of partial dislocations along twin boundaries. This process contributes significantly to the shear strain and is a hallmark of the exceptional ductility observed in nanotwinned metals under shear [5].

Interplay Between Bending and Shear Mechanisms

While bending and shear are distinct loading modes, in practical applications nanowires are often subjected to complex stress states that involve both bending and shear components. The local stress distribution in a bent nanowire inherently produces regions of high shear near the outer fibers. As a result, a nanowire undergoing bending may initially experience elastic curvature, followed by the onset of shear-driven dislocation activities, including TBS and conventional slip [28].

The competition between bending-induced GND accumulation and shear-induced partial dislocation nucleation defines the overall plastic response. In larger nanowires, bending tends to produce a gradient in dislocation density, with the tensile side accumulating more mobile dislocations. In contrast, in thinner nanowires the free surfaces not only promote dislocation escape (leading to dislocation starvation) but also enhance surface diffusion, which, as noted, can trigger shear softening mechanisms. These interrelated processes imply that the deformation behavior of nanowires is highly size dependent and that the mechanisms activated under pure bending may be modified significantly by superimposed shear stresses [29].

Moreover, micro-bending experiments coupled with in situ imaging techniques have provided clear evidence that, in many cases, the onset of plasticity is not a homogeneous process but rather a localized phenomenon. For example, Weber et al. observed that bending leads to localized regions of high strain that favor the nucleation of dislocations and twin boundaries, which then interact and evolve under the influence of both bending and shear components. This localized plasticity is further modulated by the nanowire's crystallographic orientation and the detailed nature of its free surfaces [20], [29].

Modeling and Simulation Approaches: The complex interplay between bending and shear induced deformation mechanisms in nanowires has motivated the development of multi-scale modeling approaches. At the continuum scale, nonlocal crystal plasticity models that incorporate strain-gradient effects have proven invaluable in predicting size-dependent behavior. These models, as advanced by Yefimov et al. [18]and later extended by Sandfeld et al. [19], use dislocation density evolution equations to capture the kinematics of plasticity in bending and shear.

At the atomistic level, MD simulations have provided critical insights into the nucleation of partial dislocations and the subsequent evolution of twin boundaries under shear. For instance, MD studies on FCC nanowires have confirmed that the activation of TBS is strongly influenced by both the intrinsic stacking fault energy and the local stress state [25]. Similarly, studies by Park et al. [27] illustrate how slip and twinning compete under different loading scenarios, revealing the sensitivity of deformation pathways to applied stress orientation.

These simulation approaches have also been combined with experimental techniques—such as in situ TEM bending tests and shear tests—to validate model predictions and elucidate the underlying mechanisms. The combined use of continuum, discrete dislocation, and atomistic models provides a robust framework for understanding the deformation of nanowires under complex loading conditions.

Five-Fold Twin Boundaries in Nanowires

Five-fold twin (FFT) structures are commonly observed in metallic nanocrystals and nanowires, particularly in face-centered cubic (FCC) metals such as gold, silver, and copper [30]. These structures form when five coherent twin boundaries (TBs) converge along a common axis, resulting in a pentagonal cross-section with intrinsic internal stress due to the crystallographic misfit [31]. The unique mechanical properties of FFT-containing nanowires, including enhanced strength, ductility, and resilience against plastic deformation, arise from their distinct deformation mechanisms under different loading conditions, such as bending, shear, and axial tension [32]. This section provides an in-depth discussion

on the deformation mechanisms associated with FFT boundaries in nanowires, with a focus on dislocation interactions, twin boundary migration, and the effects of extreme loading conditions.

Formation and Stability of FFT Boundaries: The formation of FFT structures is influenced by sequential twinning and the decomposition of high-energy grain boundaries [30]. HRTEM and MD simulations have revealed that FFTs can nucleate through dislocation-driven twinning or annealing-induced grain boundary migration [31]. The presence of a 7.33° angular mismatch in FFT structures introduces intrinsic disclination stress, which significantly alters their mechanical response under deformation [32].

Sequential Twinning and Grain Boundary Decomposition: During mechanical loading, FFTs can form via the successive emission of partial dislocations on different twinning systems [30]. Studies on gold nanocrystals under bending have shown that sequential partial dislocation slip leads to the transformation of stacking fault bundles into a fully developed FFT [31]. Additionally, grain boundary decomposition at the junctions of multiple twins plays a critical role in stabilizing the FFT structure by reducing excessive strain energy [32].

Twin boundaries in FFT structures serve as both obstacles and facilitators of dislocation motion. Unlike conventional coplanar nanotwins, which promote dislocation slip along predefined planes, FFT structures introduce multiple intersecting twin boundaries that create complex dislocation reactions. MD simulations indicate that when a dislocation approaches an FFT junction, it may either be absorbed, transmitted, or undergo cross-slip depending on the local stress state [31]. This results in enhanced strain hardening compared to single twin structures, as dislocation pile-up at twin junctions delays yielding and increases strength [30].

Role of Intrinsic Stress Fields: The inherent stress field of FFTs influences their deformation behavior significantly [33]. Unlike conventional twin boundaries that act as strong barriers to dislocation motion, FFTs introduce additional complexity due to the accumulation of internal stress along the five-fold junction [31]. This stress can facilitate dislocation cross-slip and climb, leading to unique deformation pathways [32]. Due to the intrinsic disclination stress, FFT structures are often more resistant to plastic deformation under uniform loading but may undergo localized deformation under extreme stress conditions, such as cyclic bending [33].

Dislocation Interactions and TBS: Recent studies on FFT metallic nanocrystals, particularly gold, reveal that their mechanical behavior is strongly influenced by how dislocations interact with complex twin boundary networks. First, dislocations are frequently impeded by twin boundaries, forming extended defects such as stacking faults or stair-rod dislocations. This barrier effect translates into higher yield strength and enhanced work-hardening capacity. Second,

cross-slip and transmission events are common: incoming dislocations may glide onto the twin boundary plane or transmit across it, governed by local stress levels and partial dislocation configurations. These events often leave residual partials behind, prompting further TB migration or rearrangement. Third, multiple TBs converging at the penta-twin "core" enable complex, coordinated deformation: dislocations entering this core can split, recombine, or trigger partial emission in neighboring twin boundaries. Such interplay can lead to core dissociation or the development of reconstructed pentagonal regions. Finally, FFT-containing nanocrystals can accommodate plastic deformation through coordinated TB movements, rather than conventional slip alone, offering both robustness and flexibility [31]. Figure 2.6 provides a closer look at these dislocation interactions in penta-twinned nanocrystals, highlighting both partial and full dislocation transmissions and the accompanying twin lamella growth or TB step enlargement under strain.

Figure 2.6. Dislocation interactions with penta-twins: (a) Dislocation impedance within a single twin subunit, leading to twin lamella growth and twin boundary (TB) step enlargement under strain. (b) Partial dislocation transmission across a TB. (c) Full dislocation transmission across a TB. White and red arrows indicate dislocation propagation and mechanical loading directions, respectively. Insets show Burgers vector circuits and FFT patterns of penta-twinned nanocrystals [31].

Climb-Induced Dislocation Annihilation and Core Dissociation: A key mechanism observed in penta-twinned metallic nanocrystals is climb-induced dislocation annihilation, particularly at the highly stressed core region where multiple TBs converge. When a dissociated dislocation, comprising a leading and trailing partial, becomes blocked at a twin boundary,

it may recombine into a compact dislocation and then climb along the boundary toward the penta-twin core. This climb process is facilitated by local stress concentrations and the availability of point defects (e.g., vacancies) that help drive dislocation motion off the glide plane. Upon reaching the core, the dislocation either annihilates or is absorbed, effectively removing it from the lattice. Meanwhile, the increased distortion at the core stimulates additional partial emissions, enabling further plastic relaxation. Over multiple climb-and-annihilation cycles, core dissociation can occur, disrupting the original pentagonal boundary arrangement and leaving behind residual defects that reshape the twin boundary configuration [32]. Figure 2.7 details this sequence of events, showing the dislocation contracting, climbing along TB1, and ultimately annihilating at the core, an event confirmed by MD simulations that also capture the ensuing partial emissions. This phenomenon accommodates plastic strain while reorganizing the fivefold structure and can lead to a partial “reconstruction” of the core region, thereby enhancing both strength and ductility in FFT nanocrystals [32].

Figure 2.7. Dislocation annihilation at the penta-twin core via dislocation climb: (a, b) A full dislocation (d1) contracts its dissociated length as it approaches TB1. Insets show the dissociated and compacted states of the dislocation. (b, c) The dislocation climbs along TB1 toward the core. (c, d) Final annihilation at the core, triggering partial emission along TB3. Insets illustrate atomic variations at the free surface. (e–h) Schematic of the dislocation mechanisms. (i–k) MD simulations confirming similar annihilation behavior, with FCC, HCP, and disordered structures marked in blue, red, and cyan, respectively [31].

Strength and Hardening Mechanisms: Nanowires with FFT structures exhibit superior mechanical strength compared to their single-crystalline counterparts (X. Wang et al., 2023). The presence of multiple twin boundaries introduces additional barriers to dislocation motion, leading to significant strain hardening. Experimental data on silver nanowires indicate that FFT-containing structures can sustain much higher stresses before yielding compared to untwinned nanowires [31].

Furthermore, FFT structures contribute to an increase in the elastic strain limit of nanowires [33]. Unlike single-crystal nanowires that typically experience brittle failure after reaching their yield strength, FFT-containing nanowires exhibit a combination of high strength and enhanced plasticity due to the ability of twin boundaries to accommodate deformation through sliding and migration [31].

Size-Dependent Deformation Behavior: The mechanical response of FFT-containing nanowires is highly dependent on their size [33]. As the diameter decreases, surface effects become more pronounced, leading to an increase in strength due to dislocation starvation. However, below a critical diameter, surface diffusion mechanisms dominate, leading to an inverse Hall-Petch effect where smaller nanowires exhibit lower strength due to enhanced surface-mediated plasticity [32].

Additionally, FFT-containing nanowires exhibit unique mechanical behavior under bending loads [33]. While single-crystal nanowires tend to experience localized fracture under bending, FFT structures allow for distributed plasticity, increasing overall flexibility and fracture resistance [31].

FFT boundaries in nanowires present a fascinating interplay between internal stress, dislocation dynamics, and mechanical robustness. Their ability to accommodate large plastic strains while maintaining high strength makes them attractive for applications in flexible electronics, nanoscale actuators, and high-performance structural materials [31]. Future research should focus on harnessing these unique deformation mechanisms to engineer nanomaterials with tailored mechanical properties. Additionally, further studies on the dynamic evolution of FFT structures under cyclic loading and extreme environments will provide deeper insights into their long-term reliability and performance [32], [33].

CHAPTER THREE: METHODOLOGY

This study employs computational simulations to investigate the deformation behavior of single-crystal metal nanowires subjected to three primary loading conditions:

1. Three-point bending
2. Top bending
3. Shear loading

A key challenge in modeling nanowire mechanics is the discrepancy between experimental timescales and computationally feasible simulations. This work employs ABC simulations, to address the inherent limitations of conventional MD in simulating long-timescale processes such as creep deformation. A comparative study between MD and ABC under conditions where MD remains applicable enables a deeper understanding of their strengths and limitations.

3.1 Simulation Methods

Molecular Dynamics

MD is a computational technique that simulates the time evolution of an N-body atomic system by numerically integrating Newton's equations of motion. Over the decades, MD has evolved into a fundamental tool in materials science, enabling researchers to probe atomic-scale processes with remarkable detail [14].

The development of MD can be traced back to early work in statistical mechanics during the mid-20th century, when researchers began simulating simple systems such as hard spheres and Lennard-Jones fluids. As computational power increased, MD evolved to simulate more complex systems—including liquids, solids, and biomolecules—thereby becoming indispensable for studying phase transitions, defect dynamics, and mechanical behavior at the atomic level [13].

Fundamentals of MD Simulations: MD simulations are based on classical mechanics, where the motion of each atom in a system is determined by solving Newton's equations of motion. In a typical MD simulation, the following key components are involved:

- Interatomic Potentials: The accuracy of MD simulations critically depends on the interatomic potentials or force fields used to model interactions between atoms. These potentials capture various contributions such as bonding interactions, van der Waals forces, and electrostatic interactions. For metallic systems, the embedded atom method

(EAM) is widely used because it captures many-body interactions and reliably reproduces bulk as well as surface properties. Other potentials, such as Lennard-Jones, Stillinger–Weber, or Tersoff, are employed depending on the nature of the material under investigation. The choice of potential is critical, as it directly impacts the accuracy and predictive power of the simulation [15].

- Integration Algorithms and Time Steps: To compute the trajectories of atoms, numerical integration algorithms—such as the Verlet or leapfrog algorithms—are used. The choice of time step is crucial; it must be small enough to accurately capture the fastest vibrational motions (typically in the femtosecond range) yet long enough to allow meaningful sampling over simulation timescales. Balancing this trade-off is essential for obtaining reliable simulation data [15].

- Thermodynamic Ensembles: Statistical ensembles in MD provide a framework for how a system exchanges energy, volume, or particles with its surroundings. Essentially, they define the conditions under which the simulation is run. The selection of the appropriate ensemble is guided by the physical conditions that one aims to replicate:
  Microcanonical Ensemble (**NVE**): In the NVE ensemble, the number of particles (N), the system volume (V), and the total energy (E) are kept constant. MD simulations in this ensemble conserve energy, making them ideal for studying isolated systems where no energy exchange occurs with the surroundings [34].
  Canonical Ensemble (**NVT**): The NVT ensemble maintains a constant number of particles, volume, and temperature. Temperature control is achieved using thermostats—such as the Nosé–Hoover thermostat—which allow the system to exchange energy with an external heat bath. This ensemble is particularly useful for exploring equilibrium properties at a defined temperature [34].Isothermal–Isobaric Ensemble (**NPT**): In the NPT ensemble, the number of particles, pressure, and temperature remain constant. Barostats, such as the Parrinello–Rahman method, dynamically adjust the simulation cell dimensions to maintain a constant pressure. This approach is important for studying systems under variable volume conditions, phase transitions, and mechanical responses to pressure [34].
  Generalized Ensembles: Beyond the conventional ensembles, generalized ensemble techniques (e.g., metadynamics, umbrella sampling, replica exchange MD) modify the sampling distribution to enhance the exploration of phase space. These methods are particularly useful for overcoming energy barriers and accessing rare events that are otherwise inaccessible in standard MD simulations [34].

- System Size and Boundary Conditions: In simulations of nanomaterials, the size of the system must be carefully considered to capture the phenomena of interest while managing computational costs. Periodic boundary conditions

are often used to mimic an infinite system, although for nanostructures such as nanowires or nanoparticles, free surfaces are explicitly modeled to preserve the characteristics of finite-sized systems [15].

MD simulations have been extensively applied to study various aspects of nanomaterials, including:

- Deformation Mechanisms: MD has provided insights into how nanomaterials deform under mechanical load, revealing the atomic-scale processes such as dislocation nucleation, surface diffusion, and phase transformations that govern their mechanical behavior [3], [15].
- Thermal Stability: The response of nanomaterials to thermal fluctuations, including melting behavior and phase transitions, has been probed with MD to understand size-dependent thermodynamic properties [15].
- Interfacial Phenomena: MD enables the study of interfaces between different materials, such as in core–shell nanowires or composite materials, where interfacial stresses can play a pivotal role in determining overall mechanical performance [15].

Challenges in Conventional MD Simulations-Time Scale Bottleneck

MD simulations are a powerful tool for exploring atomic-scale phenomena, but they are inherently limited by the timescales they can access. One of the principal challenges in conventional MD arises from the necessity to resolve the fastest atomic motions in a system. Since individual atomic vibrations occur on the order of femtoseconds (10^{-15} seconds), the integration time-step used in MD must also be on this timescale to accurately capture the dynamics. This requirement means that even when simulations run for millions of integration steps, they only cover time spans in the range of nanoseconds to microseconds [16], [17].

This fundamental timescale bottleneck severely restricts the scope of processes that can be studied using conventional MD. Many interesting and critical physical phenomena occur over much longer timescales—often spanning microseconds to seconds or even longer. For example, processes such as creep, long-range diffusion, protein unfolding, and grain boundary dynamics unfold over timescales that are orders of magnitude longer than what standard MD can capture. As a result, these phenomena remain largely inaccessible to conventional MD simulations [16], [17].

The inability to bridge this vast gap between the rapid atomic vibrations and the slow, large-scale processes limits the application of MD in several key areas. While MD excels in providing detailed insights into fast, local events, it struggles to capture the evolution of systems where collective phenomena or rare events dominate the behavior. This limitation is a driving force behind the development of enhanced sampling techniques, which aim to overcome the timescale bottleneck

by accelerating the exploration of the potential energy landscape and enabling the study of events that occur over much longer periods [16], [17].

Long Timescale Methods

To address the timescale limitation of conventional MD, researchers have developed a variety of long timescale methods. Some approaches involve artificially increasing temperatures, stresses, or strain rates to accelerate system evolution. However, these methods can distort the underlying physics, leading to inaccurate predictions of material behavior. More sophisticated approaches have therefore been devised to extend MD simulation timescales without compromising accuracy [16], [17].

Long timescale atomistic methods can generally be classified into two broad categories: Potential Energy Surface (PES) exploration and Accelerated MD.

PES Exploration Methods: These techniques rely on finding transition states and energy barriers between local minima on the PES. Examples include:

- Metadynamics: Uses a history-dependent biasing potential to push the system out of local minima, allowing exploration of new states [16].
- Activation-Relaxation Techniques (ART): Identifies saddle points on the PES by perturbing the system and relaxing it toward neighboring minima [16].
- Dimer Method: Efficiently searches for transition states without requiring Hessian calculations [16].

Accelerated MD Approaches: These methods modify the equations of motion to allow for longer time steps or enhanced sampling of rare events. Examples include:

- Hyperdynamics: Introduces a bias potential to reduce the effective energy barriers between states, accelerating transitions [16].
- Parallel Replica Dynamics: Uses multiple independent replicas of the system to accelerate rare event sampling [16].
- Temperature-Accelerated Dynamics (TAD): Raises the system temperature and extrapolates results back to lower temperatures to predict long-term evolution (Yan et al., 2016).

Many of the PES or accelerated MD methods have originated to solve problems involving diffusion, chemical reactions, glass transitions, where mechanically driven system evolution is not the primary physics of interest. The ABC Sampling Method was motivated by the need to study mechanically driven systems directly.

Understanding the Potential Energy Landscape (PEL)

A central concept in both MD and enhanced sampling methods is the potential energy landscape (PEL), which is a multidimensional surface representing the energy of a system as a function of its atomic coordinates, as shown in figure 3.1. The PEL is a fundamental tool for understanding the thermodynamic and kinetic properties of materials.

Figure 3.1: The Potential Energy Surface, or PES, is an invisible dimension of our reality, it describes all possible configurations of a system. The PES is a 3N-dimensional landscape where each point corresponds to a specific configuration of all N atoms. Local minima on this surface represent stable states, while saddle points represent transition states. The ABC method ‘climbs’ this PES by surmounting energy barriers, enabling us to capture important transition events [35].

Key Features of the PEL

Local Minima: These are locations on the energy landscape where the system can reside in a relatively stable state. Each local minimum corresponds to a particular atomic configuration that is energetically favorable [35].

Energy Barriers: The energy differences between local minima and the saddle points (transition states) separating them are known as energy barriers. These barriers determine the rate at which a system can transition from one configuration to another. Higher energy barriers correspond to less frequent transitions and longer timescales for events such as dislocation nucleation or phase transformations [35].

Global Minimum: The lowest point on the PEL is the global minimum, representing the most stable configuration of the system under given conditions [35].

X and Y-Axis (Reaction Coordinate or Collective Variable): Represents a reaction coordinate or a collective variable that traces the progression of the system from one configuration to another. This might involve atomic displacements or other order parameters that effectively describe transitions [35].

Z-Axis (Potential Energy): Represents the potential energy of the system corresponding to each configuration along the reaction coordinate. Peaks denote energy barriers, while valleys indicate stable or metastable states [35].

The Autonomous Basin Climbing (ABC) Method

ABC is a PES-based approach designed to systematically explore energy landscapes and identify transition pathways over long timescales. Originally proposed by Yip et al. in 2009, ABC has been used to study various slow processes, including diffusion, yield stress effects, grain boundary dynamics, and viscous relaxation [26], [36].

ABC Workflow

1. Initialization, begin with the system relaxed at a local energy minimum on the potential energy surface (PES).

2. First penalty function application, figure 3.2, introduce a penalty function (usually Gaussian-shaped) centered at the current minimum, with a small random half-width and height. At this point, there are two potential energy surfaces: the original PES and the augmented energy surface that includes the penalty [16].

Figure 3.2, after the first penalty function is applied, there will be a augmented energy surface that includes the penalty, and the original PES [16].

3. Relaxation, figure 3.3, minimize the augmented potential energy surface (modified PES, the original energy plus the sum of applied penalties) to locate the next local minimum on this augmented energy surface.

Figure 3.3: The system is minimized on the augmented potential energy surface following each application of a new penalty function. The system may be minimized to a new local minimum (middle and right) or remains in the original basin (left) [16].

4. Check for True Local Minimum, figure 3.4, check whether the current configuration is a true local minimum 3, which satisfies the following two criteria: vanishing force and nonzero distance away from all the previous true local minima.

    a) If a true local minimum is found, the algorithm backtracks along the last minimization path to locate the saddle point configuration. Then update the current penalty function selection rule using the displacement and the energy difference between the new local minimum and the corresponding saddle point.
    b) If a true local minimum is not found, the current penalty function selection rule is kept unchanged.

Figure 3.4: If a true local minimum is found, the penalty function selection rule is updated using the measured displacement and energy difference between the new minimum and the saddle point. This adjustment accelerates future escapes from this basin [16].

5. Sequential penalty function addition, the algorithm adds a new penalty function with an updated or unchanged rule, depends on the outcome of the previous step.

6. Overlap check, figure 3.5, after new penalty function is added, the algorithm checks whether it overlaps with any previously applied functions. Overlap is determined by comparing the distance between centers relative to the sum of their half-widths. For any two penalty functions, if the 3N-D distance between their centers is smaller than the sum of their half-widths, these two closely positioned penalty functions will be replaced by a combined penalty function.

Figure 3.5: With each new penalty function, the algorithm checks for overlaps by comparing the distance between centers relative to the sum of their half-widths. If two functions overlap, they are merged into a new one, which reduces memory use and computational cost. The combined function then replaces the previous overlapping ones [16].

7. Repeat Step 3 – 6, Until a sufficiently large configurational space has been sampled.

Figure 3.6: This flowchart summarizing the ABC workflow.

ABC allows for systematic exploration of transition states and activation barriers, making it particularly useful for studying mechanical deformation at experimentally relevant strain rates. Instead of tracking every atomic vibration like MD, ABC uses energy-based strategies, specifically, penalty functions, to ‘lift’ the system out of local energy basins. This

directed exploration targets significant transitions, or metabasin escapes, whereas MD naturally samples the entire 3N-dimensional PES, including many fluctuations that may not affect long-term behavior [16], [36], [37].

ABC	Conventional MD
• Directed PES Exploration, ABC modifies the PES by adding penalty functions that help the system escape from local minima. • "Uses" the energy as an extra dimension to focus on significant transitions. • Pinpoints metabasin escape events without having to follow every intermediate atomic vibration.	• **Full PES Exploration,** MD naturally explores the 3N-dimensional PES. • Many configurations and small fluctuations are sampled may not be relevant for long-term behavior. • MD provides a very detailed view of the system's dynamics, capturing all atomic movements.

Challenges and Limitations of the ABC Method

Computational Efficiency: As the ABC method explores the potential energy surface (PES), it accumulates many penalty functions to prevent re-sampling already explored regions. This buildup increases computational cost and memory usage. Although strategies like the SLME approach reduce this overhead by merging redundant penalty functions, scaling the method to larger systems remains challenging [36], [37].

PES Resolution and Parameter Selection: The effectiveness of the ABC method relies on the careful selection of penalty function parameters (such as height and width). If these parameters are too large, the method may overlook important details in the energy landscape; if too small, it may require an excessive number of steps to drive transitions. Currently, there isn't a systematic, automated way to choose these parameters dynamically, which affects both the accuracy and efficiency of the method [36], [37].

Entropic Effects: ABC focuses on the potential energy landscape without directly incorporating entropy, which is a critical component of the free energy, especially at higher temperatures or in soft materials. While approaches like Transition State Theory (TST) and Kinetic Monte Carlo (KMC) can help estimate dynamic properties, fully accounting for entropic contributions remains an unresolved issue [16], [36].

One-Dimensional PES Exploration: Traditional ABC and ABC–SLME methods explore the PES in a largely one-dimensional fashion, following a single escape pathway from a local energy basin. This can lead to an incomplete picture

of all possible transition routes and may result in an overestimation of transition times, as alternative, possibly more favorable paths are ignored. Extended methods (like ABC-E) address this by sampling multiple pathways but at increased computational cost [16], [36].

Length Scale Limitations: The current implementation of ABC methods is limited to systems of relatively modest size (typically tens of thousands of atoms). This restriction hinders the application of ABC to larger, more realistic materials where many-body interactions occur over larger length scales. Overcoming this limitation would be necessary for broader practical use [16], [36].

The ABC method represents a promising tool for extending atomistic simulations to experimentally relevant timescales. By systematically exploring the PES and identifying transition pathways, ABC overcomes the limitations of conventional MD and provides valuable insights into slow material processes. Despite its computational demands, ABC continues to be refined and integrated with other advanced sampling techniques to enhance its accuracy and applicability. Future developments will likely focus on improving its efficiency and extending its use to more complex materials and mechanical systems.

3.2 Simulation Setup

To investigate the deformation mechanisms of metallic nanowires under bending and shear loading, computational simulations were performed using MD and ABC methods.

Simulation Framework

All simulations were conducted using LAMMPS (Large-scale Atomic/Molecular Massively Parallel Simulator) with the Embedded Atom Method (EAM) potential to model interatomic interactions. The simulations involved:

- Metallic Nanowires: Silver (Ag) and Gold (Au) nanowires.
- Periodic Boundary Conditions: Applied selectively depending on deformation mode.
- Force Field: eam/alloy potential, validated for FCC metals.
- Temperature Control: Nosé-Hoover thermostat for MD; slow energy relaxation in ABC.

The nanowire models were either created within LAMMPS or imported from atomic structures created in Atomsk.

Nanowire Model and Simulation Box

The metallic nanostructures were modeled as single-crystal FCC nanowires (Bending) and nanostructures with repeating pre-existing twinboundaries parallel to the loading direction (Shear), with dimensions tailored to the experimental conditions. The orientation was chosen to align with realistic crystallographic configurations.

Loading Conditions and Deformation Setup

1. Three-Point Bending

Objective: Investigate creep behavior under sustained bending load.

Setup: Fixed constraints at two support regions. An external pushblock applied force at the midpoint.

2. Top Bending

Objective: Investigate creep behavior under sustained bending load.

Setup: An external pushblock or a designated section within the nanowire (topend) applied gradual force on the top of the nanowire.

3. Shear Loading

Objective: Study atomic-scale processes like stacking fault formation and TBS.

Setup: Shear forces applied parallel to direction of the twinboundaries exist in the nanostructures.

Loading	Nanowire Type	Crystal Orientation	Size
3 Point Bending	Au Single Crystal Nanowire (Cylindrical)	x $[1\bar{1}0]$, y $[11\bar{2}]$, z [111]	Diameter: 4.2 nm Length (z): 33.8 nm
			Diameter: 5.2 nm Length (z): 42.4 nm
			Diameter: 7.2 nm Length (z): 59.4 nm
Top Bending	Au Single Crystal Nanowire (Cylindrical)	x $[1\bar{1}0]$, y $[11\bar{2}]$, z [111]	Diameter: 4.6 nm Length (z): 17.0 nm
			Diameter: 7.6 nm Length (z): 22.6 nm
	Au Single Crystal Nanowire (Rectangular)	x $[\bar{1}\bar{1}2]$, y $[1\bar{1}0]$, z [111]	Width (x, y): 2.4 nm Length (z): 14.5 nm
		x $[1\bar{1}0]$, y [110], z [001]	Width (x, y): 2.6 nm Length (z): 14.6 nm
			Width (x, y): 2.2 nm Length (z): 9 nm
Shear	Ag Rectangular Nanowire with repeating twin-boundaries	x $[1\bar{1}0]$, y $[11\bar{2}]$, z [111]	Width (x): 16 nm Width (y): 10 nm Length (z): 29.3 nm

Table 3.1 presents the dimensional and crystallographic orientation properties of the nanowires modelled for various loading conditions.

Identifying the Forces: A central objective of this study is to isolate long-timescale deformation mechanisms, particularly creep, which lie beyond the reach of conventional MD simulations. To achieve this, a systematic approach was adopted to identify force values that induce creep behavior in ABC simulations without triggering immediate plasticity in MD. MD serves as a screening tool to determine the critical force thresholds, ensuring that the selected forces remain below the yield point in MD yet are sufficient to activate thermally driven, long-term deformation processes in ABC. This strategy enables targeted investigation of creep while maintaining consistency across simulation methods.

Step 1: Establishing a Baseline with MD Simulations

- A constant force is applied to the nanowire in MD, starting from an initial force value (F_0).
- After the simulation is completed, the atomic structure is analyzed using Common Neighbor Analysis (CNA) in Ovito to check for plastic deformation (dislocation nucleation, twin boundary formation, etc.).
    a) If no plastic deformation is observed, the force is incrementally increased until plasticity appears.
    b) If plastic deformation is observed, the force is incrementally decreased until plasticity disappears.

Step 2: Determining the Plasticity Threshold Force (F^t)

- The plasticity threshold force (F^t) is defined as the smallest force value that induces dislocations in MD.
- This threshold is determined by gradually adjusting the force in small increments (e.g., ±0.0001 to ±0.05 force units) until a transition is observed.

Step 3: Selecting Forces for ABC Simulations

- Forces below the plasticity threshold ($F < F^t$) are selected for ABC simulations.
- Typical values chosen are slightly below F^t (e.g., $F = 0.8F^t$, $0.9F^t$), ensuring:
    a) The applied force is high enough to induce deformation over long timescales.
    b) The applied force is low enough to prevent immediate plasticity, ensuring the deformation observed in ABC corresponds to creep behavior.

Step 4: Running ABC Simulations to Capture Creep

- The nanowire is simulated using ABC under forces selected from Step 3.
- If deformation is observed in ABC at forces where MD showed no plasticity, this confirms that ABC captures long-term creep mechanisms that MD cannot.

This method ensures that the deformation observed in ABC is due to creep rather than conventional plasticity, allowing for a direct comparison between the two approaches. The force selection process effectively isolates the regime where creep deformation occurs while excluding forces that lead to instantaneous dislocation motion in MD.

Simulation Parameters: The ABC simulation is controlled by a set of parameters that define how the system explores its potential energy surface, as shown in figure 3.7 and explained in table 3.2.

```
#ABC group omega sigma wstart  nkeep  temp (etol  ftol  maxiter maxeval)
abc  move   10    500   10.0   10000   300    0     0.05   400     400
```

```
 maxpf  ftol    ebarrier  dmin  randpf Bcombine   pert   keep_lm ndump
300000   5.0e-4    4.0    0.15   38353    1     1.0e-3        10       1
```

Figure 3.8 shows the format of the commands used in the ABC simulations of this work.

Parameter	Description	Values Used in This Work
group	The group of atoms subjected to ABC (e.g., "move" indicates the moving atoms).	move
omega	Scaling factor for penalty function application, influencing how strongly the system is guided away from previously visited minima.	10
sigma	Standard deviation for the penalty function smoothing, which affects how broadly the penalty function influences the system.	500
wstart	Initial weight assigned to penalty functions, controlling their impact in the early simulation stages.	10
nkeep	The number of penalty functions to retain in memory, limiting excessive accumulation and maintaining computational efficiency.	10000
temp	Temperature of the simulation (in K), influencing the thermal activation of atomic transitions.	300
etol	Energy tolerance for minimization, defining convergence criteria for local minimization steps.	0
ftol	Force tolerance for minimization, determining how small the forces must be before the system is considered at equilibrium.	0.05
maxiter	Maximum number of iterations for minimization algorithms.	400
maxeval	Maximum number of force evaluations allowed for minimization.	400
maxpf	Maximum number of penalty functions that can be applied during the ABC search.	300000
ftolerance	Force threshold used to determine if a configuration is a local minimum.	5.0e-4
ebarrier	Energy barrier threshold for detecting valid transitions between states.	3.0-5.0

dmin	Minimum displacement between two local minima to ensure they are distinct states.	0.15
randpf	Random seed used for penalty function application, introducing stochasticity in the search.	23455
Bcombine	Determines whether closely spaced penalty functions should be merged to avoid redundancy.	1
pert	Magnitude of perturbation applied to the atomic positions during local energy minimization.	1.0e-3
keep_lm	Number of local minima stored for subsequent analysis.	10
ndump	Frequency of atomic configuration dumps for visualization and further analysis.	1-10

Table 3.2: Explanation of ABC parameters, and the values used in this works.

CHAPTER FOUR: RESULTS AND DISCUSSION

In this work, the deformation behavior of silver and gold nanowires under diverse mechanical loading conditions was investigated using two simulation approaches: MD and ABC. The study encompasses various bending tests—including top bending and three-point bending—as well as shear loading experiments with forces applied along different directions. These investigations reveal that the deformation mechanisms in metal nanowires are highly anisotropic and strongly dependent on factors such as loading direction, specimen orientation, and boundary conditions. Overall, the results provide detailed insights into the size-dependent and orientation-specific mechanisms governing plastic deformation in nanowires.

4.1 Bending Tests

4.1.1 Top Bending along z = [111] (with x=$[\bar{1}\bar{1}2]$ and y=$[1\bar{1}0]$)

Top-bending tests on silver nanowires oriented along z= [111] (with x=$[\bar{1}\bar{1}2]$ and y=$[1\bar{1}0]$) were conducted using both ABC and MD simulations. For this particular type of top bending tests, the simulations were performed under applied forces ranging from F = 0.0015 to F = 0.0018. The nanowire model used had dimensions of width (x, y): 2.4 nm and length (z): 14.5 nm, and the simulations were carried out at a temperature of 300 K. Despite applying identical boundary conditions, the two methods showed markedly different outcomes. In MD, the nanowire remained in an elastic state, exhibiting increased curvature under bending but no visible plastic defects such as stacking faults or twins. By contrast, the ABC simulations revealed pronounced plastic deformation, evidenced by the nucleation of two-atomic-layer planar defects near the bottom region, where the wire was fixed in place.

Figures 4.1(a)-(c) present three consecutive snapshots from ABC-based top-bending simulations, while Figure 4.2 (a) and (b) depicting the corresponding MD results under identical boundary conditions and forces. These figures correspond to a simulation where the applied force was F = 0.0015. In the visualizations shown, the outermost layer of atoms has been removed to better reveal the internal deformation structures. Blue atoms represent atoms in the face-centered cubic (FCC) lattice, while yellow atoms correspond to atoms in the hexagonal close-packed (HCP) lattice, highlighting the formation and evolution of stacking faults and associated defects.

In Figure 4.1(a), minor bending yields two distinct, two-atomic-layer planar defects that appear near the bottom (fixed region). OVITO visualization confirms that these defects extend entirely through the cross section in both the x and y directions, indicating genuine stacking faults rather than surface steps. In Figure 4.1(b), the same stacking faults persist

without additional slip-system activation, but the wire's curvature becomes noticeably larger. As bending continues, Figure 4.1(c) shows that the nanowire in the ABC model develops multiple additional stacking faults, each traveling across both the x and y directions, culminating in more pronounced curvature and a broader distribution of planar defects. These findings are consistent with established behaviors in top-bending simulations of FCC nanowires, where partial dislocations glide along {111} planes, leaving behind stacking faults that can evolve into deformation twins under sustained plastic flow. In many bending scenarios, dislocations preferentially nucleate at the fixed bottom region, where the stress concentration is highest [38].

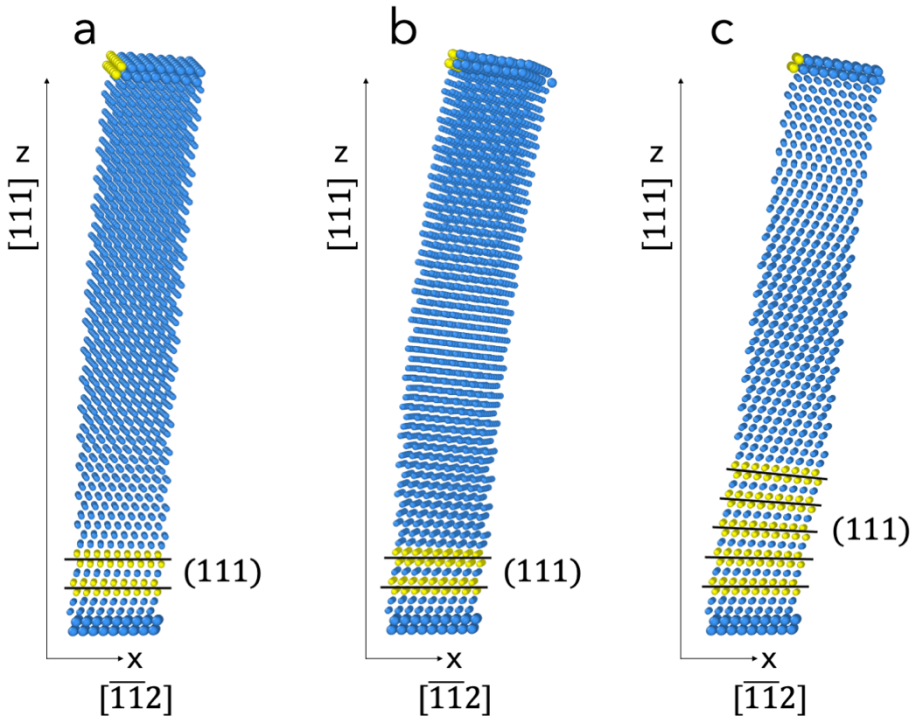

Figures 4.1(a)-(c), ABC Simulation Images. (a) At this early stage of bending, the silver nanowire displays slight curvature, with its bottom layers fixed. Two distinct two-atomic-layer defects appear at the clamped base. OVITO common neighbour analysis reveals these defects span the entire cross section, fully developed stacking faults rather than surface steps. The remaining lattice remains largely defect-free. (b) As bending intensifies, overall curvature increases, shows an elevated strain level. The same two-layer stacking faults remain. No new slip systems are activated. (c) Under greater strain, the nanowire bends sharply near the bottom. Multiple additional stacking faults emerge in both the x and y directions. These new stacking faults traverse the entire cross section. The shift from a few to numerous planar defects illustrates escalating plasticity as the wire endures sustained bending.

MD simulations are employed to investigate atomic-scale behavior over extremely short timescales, typically spanning nanoseconds to microseconds. Within such limited temporal regimes, atomic diffusion, characterized by the long-range migration of atoms, is effectively frozen and thus does not manifest during the simulation. As a result, plastic deformation captured by MD must proceed through non-diffusive mechanisms, such as the immediate nucleation of dislocations across relatively high energy barriers [17].

Conversely, ABC is specifically developed to simulate rare-event phenomena occurring over substantially longer timescales, ranging from milliseconds to seconds or beyond [16], [37]. In these regimes, atomic diffusion becomes a critical factor, permitting localized atomic rearrangements that can substantially reduce the energy barriers for plastic deformation processes, including dislocation nucleation [39]. Accordingly, ABC simulations reveal that the presence of diffusion can significantly facilitate dislocation nucleation at lower applied stresses compared to MD simulations, thereby offering enhanced insight into deformation mechanisms operative under experimental or service conditions.

This distinction is further exemplified in the MD simulation results presented in Figures 4.2(a) and 4.2(b), where the nanowire remains free of any stacking faults or dislocation traces. Under the specific MD parameters employed, the nanowire persists within the elastic regime throughout the simulation, indicating that the critical stress required for the nucleation of partial dislocations, and the subsequent onset of plastic flow, has not been reached.

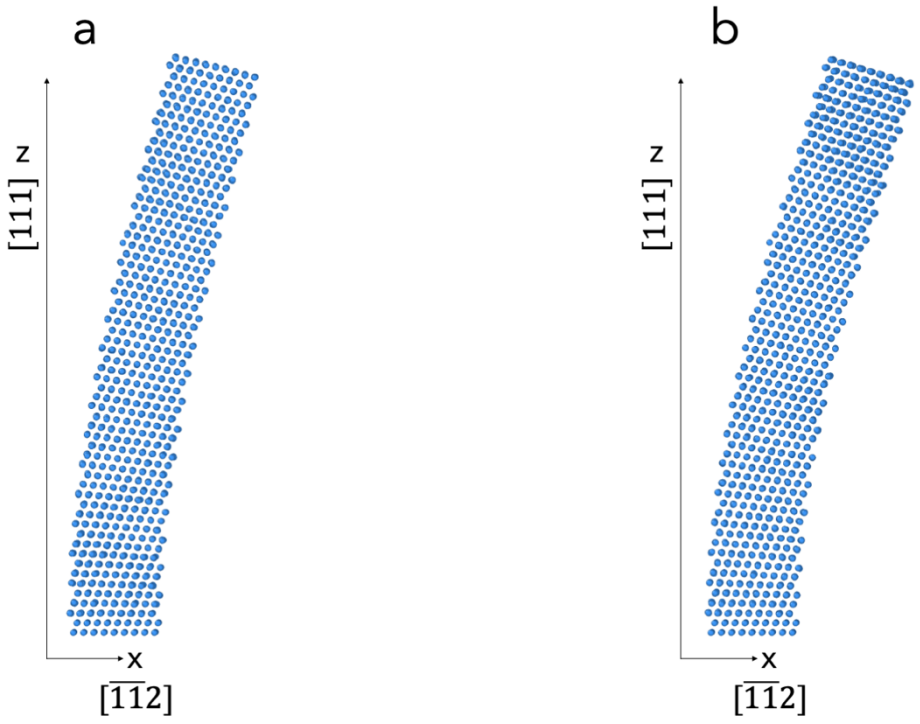

Figure 4.2 (a) and (b). In contrast to the ABC results, the MD snapshots exhibit no sign of plastic deformation. While the same boundary conditions and load parameters are applied, the nanowire simply bends elastically.

4.1.2 Top-Bending Simulations With [001] Orientation and FFT Formation

In this second series of "top-bending" simulations, the nanowires were oriented along the z = $[001]$, with x = $[1\bar{1}0]$ and y = $[110]$. The nanowires had a cross-sectional width of approximately 2.6 nm along both x and y, and an overall length of 14.6 nm along z. Simulations were conducted at a temperature of 300 K, using both the Autonomous Basin Climbing (ABC) and Molecular Dynamics (MD) approaches across a broad range of applied forces in the $[1\bar{1}0]$ direction.

Under forces calibrated to produce purely elastic bending in MD (F = 0.0003 - 0.0004), where no plastic deformation was observed, the ABC simulations demonstrated that, rather than achieving pronounced macroscopic curvature, the deformation was predominantly accommodated through the nucleation and growth of partial-dislocation–driven twins. In these cases, despite the nominal objective of bending the nanowire, plasticity mechanisms were activated through local defect formation.

At higher applied force levels (F = 0.0014 - 0.0018), both simulation methods exhibited the spontaneous onset of plasticity, characterized by the formation of fivefold twin (FFT) boundary structures. In the atomic visualizations of both ABC and MD simulation presented, the outermost atomic layer was removed to more clearly reveal the internal deformation structures. Green or blue atoms correspond to those retaining a FCC lattice environment, while red or yellow atoms represent atoms adopting a HCP configuration, highlighting the regions of stacking faults and twin formation.

Low Forces (Forces Calibrated for Elastic-Only MD Simulations)

At low applied forces, deformation is dominated by partial dislocation-mediated twinning rather than by macroscopic bending. In FCC metals such as silver, plastic deformation typically proceeds via partial dislocations on {111} planes with ⟨110⟩ slip directions. For a nanowire oriented along $[001]$ loading along the x = $[1\bar{1}0]$ direction generates high resolved shear stresses on diagonally intersecting {111} planes, thereby promoting slip and twin formation instead of large-scale bending.

In FCC metals, the formation of deformation twins is generally preceded by the nucleation of isolated stacking faults, initiated through the glide of leading partial dislocations on {111} planes [40]. With continued application of stress, successive partial dislocations glide on adjacent {111} planes, causing the stacking faults to thicken and coalesce into coherent twin structures [40]. After twin formation, twin boundaries are not static; they can migrate dynamically through

the nucleation and glide of additional twinning partials, providing an efficient mechanism for strain accommodation during plastic deformation [40]. This twinning evolution and twin boundary migration behavior have been widely reported in both experimental and computational studies.

The ABC simulations vividly capture this behavior at an applied force range of F = 0.0003 – 0.0004, while the corresponding MD simulations, under identical loading conditions, exhibit purely elastic responses without any evidence of defect nucleation. The progressive evolution of the twinning mechanism under these conditions is illustrated through the sequential ABC simulation (with applied force F=0.0003) snapshots presented in Figures 4.3(a)-(e).

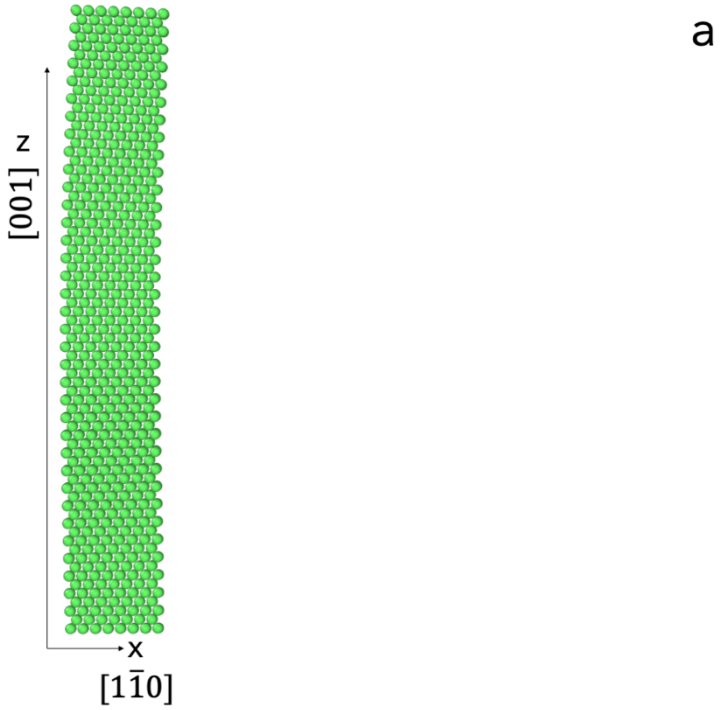

Figure. 4.3(a): The undeformed wire is intact, with no slip or faulting. A "top-bending" boundary condition is imposed by driving the top region along $[1\bar{1}0]$ and fixing the bottom region.

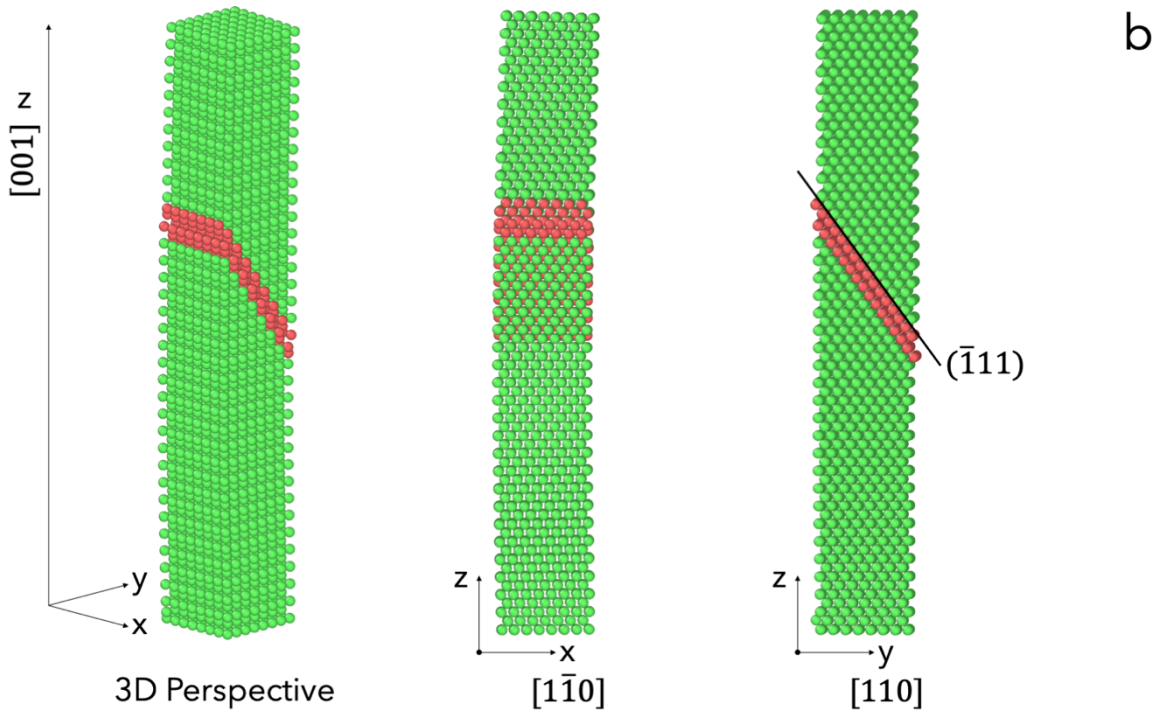

Figure. 4.3(b): Beyond a threshold, the first planar defect emerges diagonally. The red layers indicate a stacking fault left by a partial dislocation on a {111} plane. Externally, the length of the wire is slightly decreased while remains mostly straight, suggesting in-plane slip is accommodating the strain.

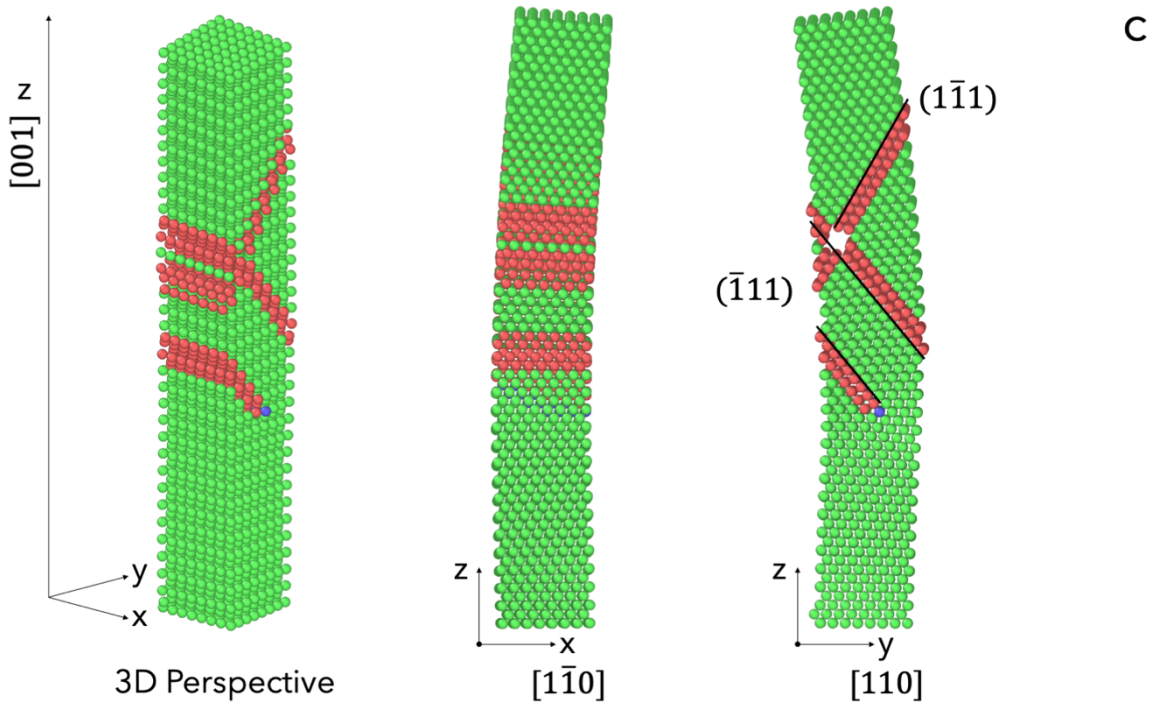

Figure. 4.3(c): The length is further reduced, while more stacking faults appear, seen as additional red atomic layers.

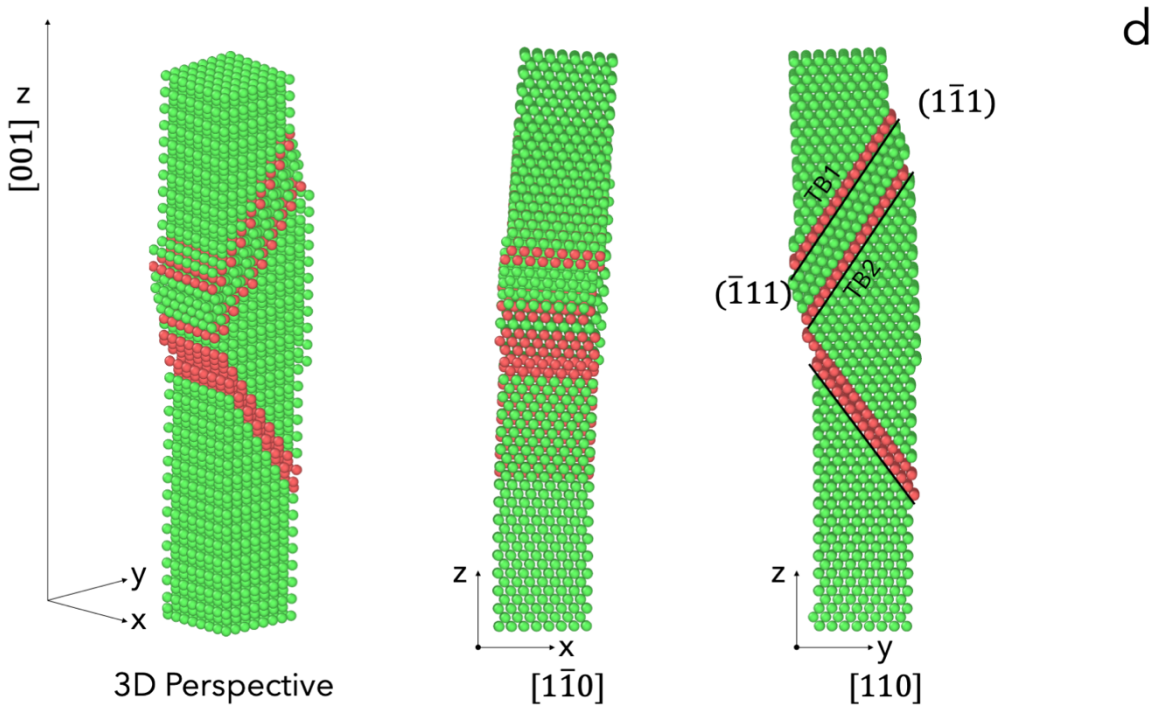

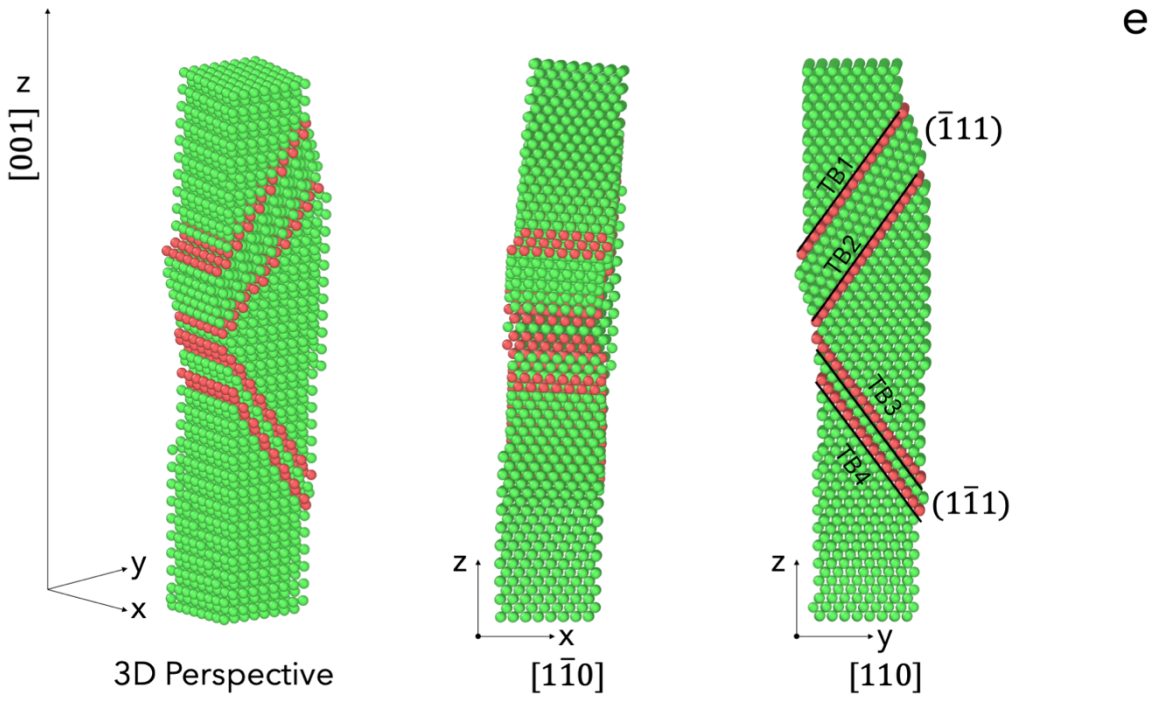

Fig. 4.3(d) and (e): Adjacent faults merge into well-defined twin boundaries. Even though this configuration was intended as a "bending test," the overall wire shape still exhibits minimal outward curvature, revealing heavy internal plastic flow through partial-dislocation activity.

Elevated Forces and FFT Boundaries

At higher applied loads (F = 0.0014-0.0018), both MD and ABC simulations produce FFT structures. In the MD simulations, figures 4.4(a)–(b), the nanowire promptly develops a characteristic star-shaped arrangement of twin boundaries, locking the structure into a multiply twinned configuration while maintaining an overall bent geometry throughout the simulation. The ABC simulations reveal a similar tendency toward FFT formation, although the phenomenon occurs with greater variability. In a representative ABC simulation under an applied force of F = 0.0014, shown in Figures 4.5(a)-(d), the nanowire transitions from an initially elastic response to localized partial dislocation slip, ultimately leading to the formation of a five-fold twinned structure. Although differences are observed in the timing of twin nucleation between the MD and ABC methods, the final star-like twin boundary configuration is consistently reproduced.

MD snapshots presented in Figures 4.4(a) and 4.4(b) illustrate that, once the applied force exceeds a critical threshold, the nanowire undergoes spontaneous plastic deformation characterized by the formation of multiple fivefold twin (FFT) boundaries. Figure 4.4(a) corresponds to an applied force of F = 0.0016, while Figure 4.4(b) presents the deformation morphology at an independently applied higher force of F = 0.0018. Notably, we observe that two distinct FFT structures tend to form at these force levels, each intersecting at a different off-centered region inside the nanowire—both are nearer the tensile side rather than the compressive side in a typical bending profile. One FFT center typically appears near the midsection, while the other resides closer to the bottom portion of the wire. Once these form, both five-fold twins persist, leaving the wire in a permanently bent and plastically deformed state throughout the remainder of the simulation.

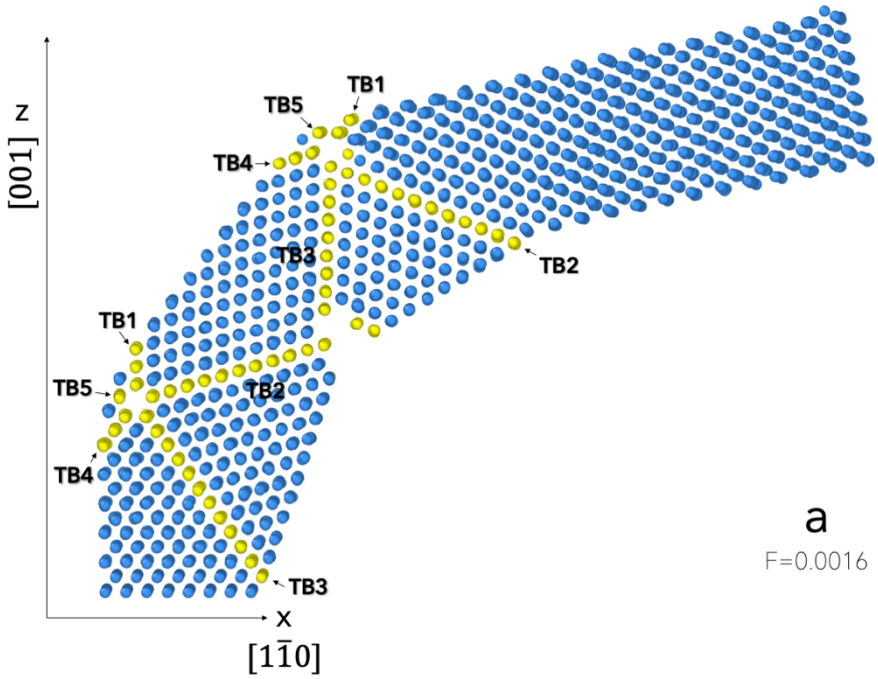

Figure 4.4 (a), MD snapshot shows a nanowire subjected to elevated bending forces (F=0.0016), resulting in the formation of two distinct FFT structures, highlighted in yellow. These FFT centers are off centered toward the tensile side, one near the midsection and the other closer to the bottom. The wire is severely plastically deformed due to the nucleation and growth of these twins but retains its final shape after their formation, indicating a stable post-yield configuration.

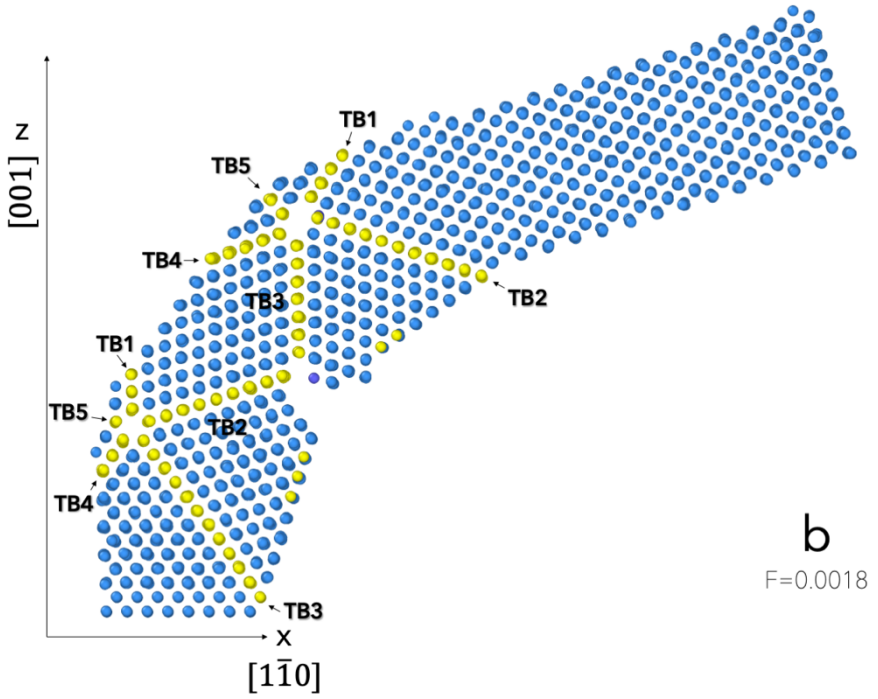

Figure 4.4 (b), at a slightly higher force level (F=0.0018), the nanowire again develops two well-defined FFT structures, marked in yellow, forming on the tensile side of the bent profile. The FFT centers are positioned similarly to those in

ABC snapshots, figure 4.5(a)-(d) provide additional insights into the formation of the five-fold twin boundary. Initially, partial dislocations nucleate at specific sites, leading to the formation of stacking faults along adjacent {111} planes. With continued deformation, these stacking faults coalesce and rearrange into a coherent twin boundary that exhibits five-fold symmetry. This observation suggests that the resolved shear stresses are nearly balanced for the nucleation of both leading and trailing partial dislocations, which in turn allows five distinct twin domains to converge at a common intersection. The formation of this five-fold twin boundary thus represents an efficient mechanism for plastic deformation, enabling the nanowire to accommodate high strains while preserving its overall structural integrity.

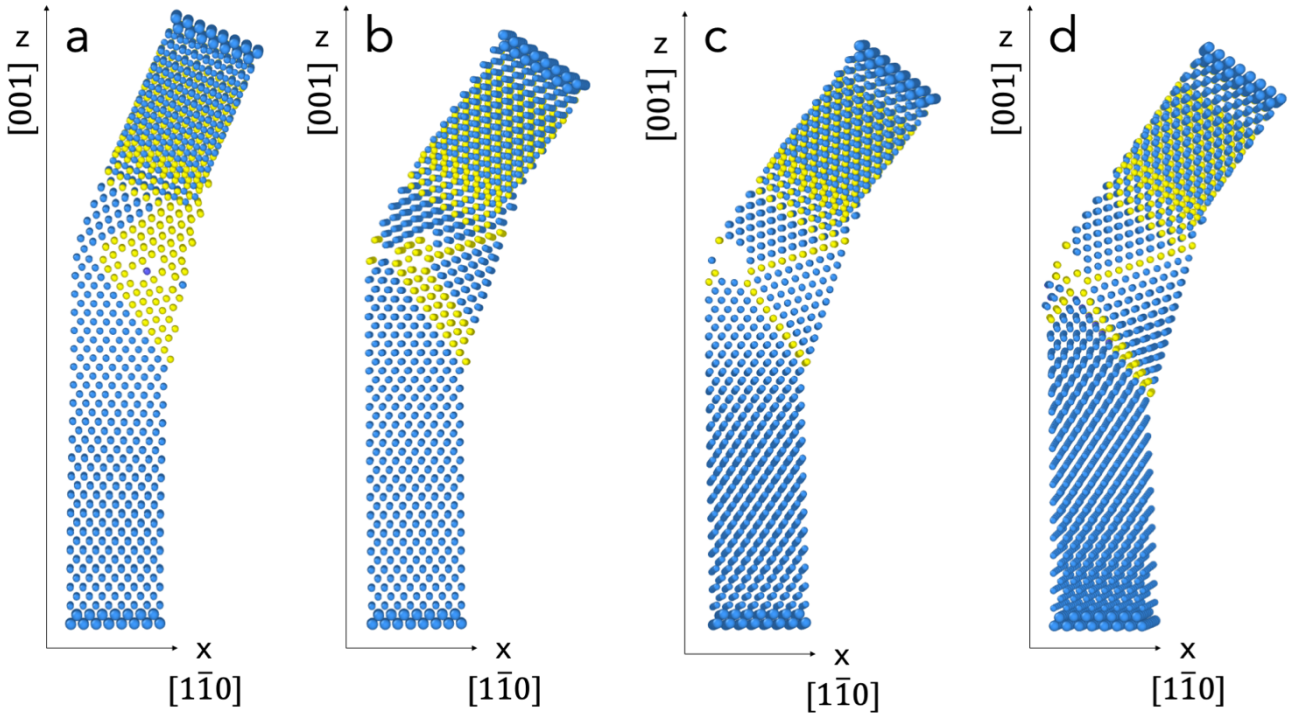

Figure 4.5: ABC snapshot of top bending test at elevated force level (F=0.0014). (a) Early nucleation stage of the five-fold twin boundary. Partial dislocations are observed initiating at distinct sites, beginning to form stacking faults along adjacent {111} planes. (b) Stacking faults continue to develop and begin to coalesce. The nascent twin boundary becomes more apparent as partial dislocations propagate along the {111} planes, suggesting that the resolved shear stresses are nearly balanced for both leading and trailing partial dislocation nucleation. (c) This snapshot captures the evolution of the twin structure. The stacking faults have merged further, and the twin boundary now exhibits a clear five-fold symmetry.

Five distinct twin domains converge at a common intersection, forming a coherent, star-shaped arrangement. (d) Fully developed five-fold twin boundary.

Collectively, these results underscore that while MD and ABC simulations differ in the precise kinetics of defect nucleation and twin boundary evolution, they converge toward a consistent final morphology characterized by the formation of a FFT structure. The emergence of FFT is a well-documented phenomenon in metallic nanowires and nanocrystals, arising from complex deformation processes including partial dislocation slip, twinning, and grain boundary reconfiguration. Prior studies have shown that FFT formation can involve intermediate structures such as icosahedral phases [41], sequential twinning slip and reversible boundary decomposition [33], and active dislocation nucleation at twin centers [42], all contributing to the structural reorganization under applied stress. Moreover, the presence of five-fold twin boundaries has been associated with enhanced mechanical properties, such as increased stiffness and yield strength, across a range of FCC metals [43].

The present observations confirm that five-fold twinning is highly sensitive to stress distribution, loading mode, and crystallographic orientation during bending deformation. The agreement between ABC and MD simulations at moderate to high loads provides critical insights into the mechanisms of plastic deformation and stability in nanoscale silver wires. These findings not only validate the capacity of five-fold twin structures to act as energetically favorable deformation products but also highlight their broader significance for designing mechanically robust nanostructured materials.

4.1.3 Three-Point Bending

In three-point bending simulations, the nanowires' long axis is oriented along z=[111], with x=$[1\bar{1}0]$and y=$[11\bar{2}]$, supported at both ends while a central load is applied along the x direction. This loading configuration generates a concentrated bending moment near the midspan region, resulting in a pronounced stress gradient across the wire diameter. Simulations were performed at a temperature of 300 K on a cylindrical nanowire model with a diameter of 5.2 nm and a length of 42.4 nm. In the atomic visualizations, the outermost atomic layer was removed to better reveal internal deformation structures; blue atoms represent those of FCC lattice, yellow atoms correspond to atoms in a HCP arrangement. Both the ABC and MD methods reveal broadly similar three-point bending behavior: the nanowire initially undergoes elastic curvature, followed by the nucleation of localized plastic deformation near the highest-stress region at midspan, and ultimately stabilizes into a plasticly bent configuration.

In the ABC simulations presented in Figures 4.6(a)-(c), a constant applied force of F = 0.0045 was used to drive bending deformation. Color-coded plastic strain distributions show that deformation localizes primarily near the midspan region. At early stages of deformation, the nanowire remains largely straight, and free of dislocations, indicating elastic bending. As strain accumulates under the applied load, localized regions of plastic activity emerge near the center loading point. These plastic regions correspond to the nucleation and glide of partial dislocations on {111} planes, leading to the formation of stacking faults. The passage of partial dislocations transforms the local atomic structure from face-centered cubic (FCC) to hexagonal close-packed (HCP), typically involving two atomic layers.

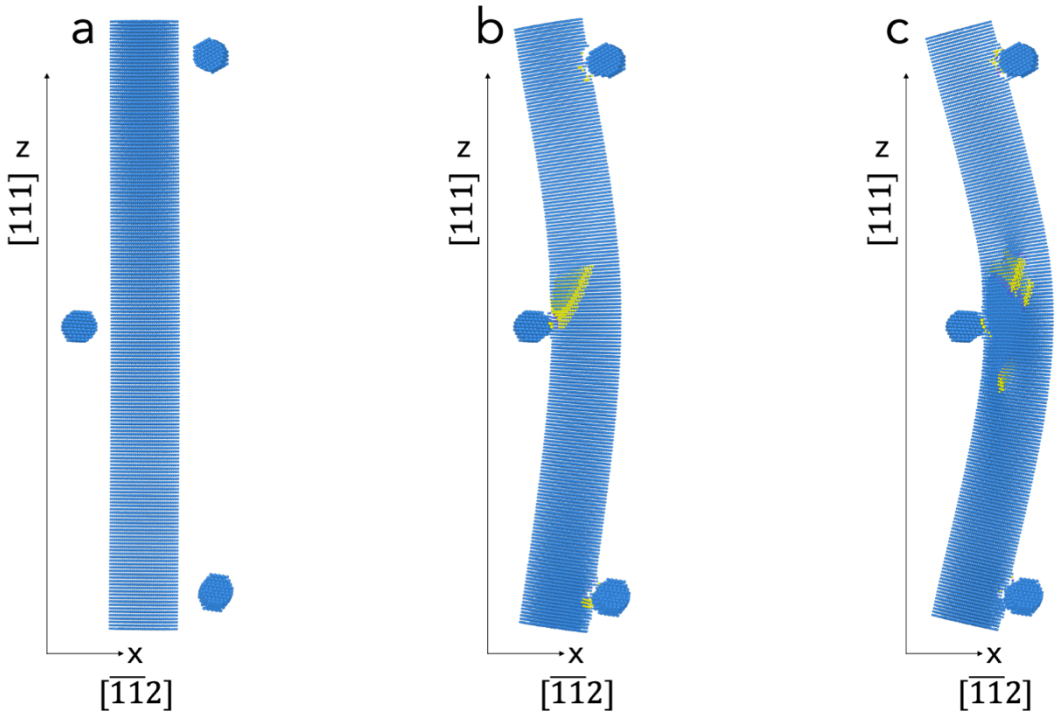

Figure 4.6: ABC Snapshots of 3 point bending test. (a) The undeformed nanowire is shown with supports near two ends and the central loading point. (b) as bending intensifies, and yellow regions mark the onset of plastic slip near the top indenter contact. Despite the classic expectation of tension-side slip, compression-driven dislocation nucleation dominates here. (c) the plastic slip bands have grown and merged into a midspan hinge.

MD simulations conducted under the same conditions as the ABC simulations described previously, figures 4.7(a)–(c), corroborate the three-point bending response but provide additional insight into the dislocation nucleation and propagation processes. As the simulation progresses and strain accumulates, partial dislocations nucleate near the center loading contact and expand diagonally across the nanowire, forming localized slip bands. With continued loading, these slip bands broaden and merge, ultimately developing into a fully formed plastic hinge that accommodates the bending deformation and stabilizes the permanent bent geometry.

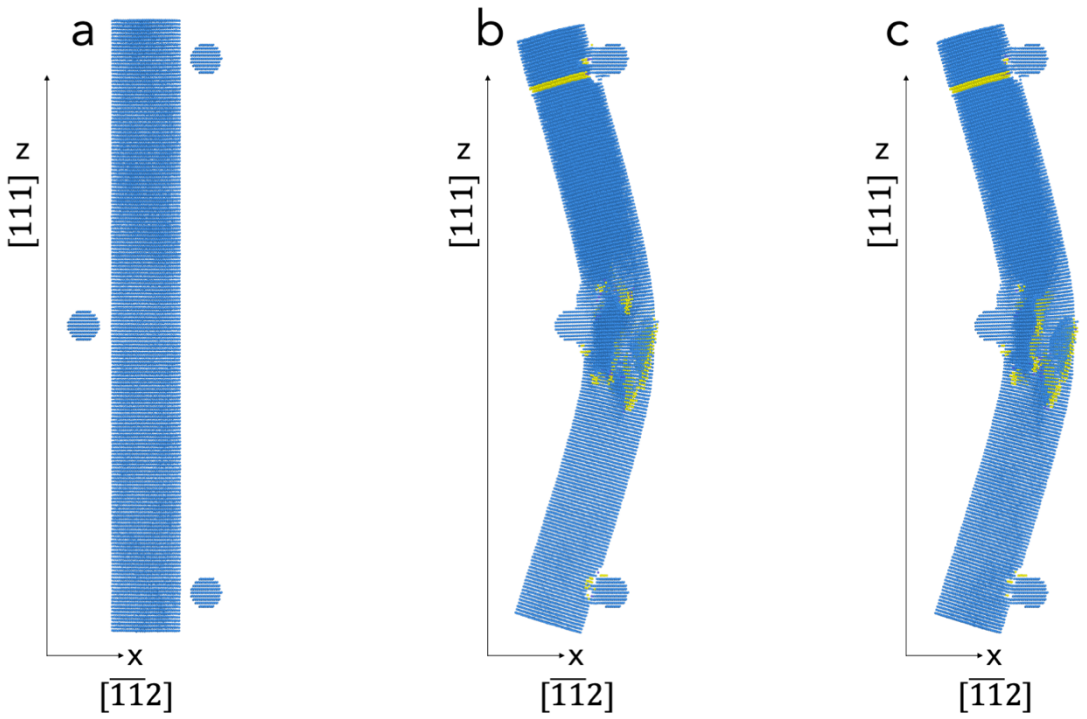

Figure 4.7: MD Snapshots of 3 point bending test (F=0.0045). (a) a fully intact, straight nanowire prior to deformation. (b) under increased load, localized plastic slip appears (highlighted in yellow). Partial dislocations begin to traverse the wire's cross section. (c) multiple dislocation bands now coalesce in the hinge region.

The stacking fault ribbons, highlighted in yellow, predominantly nucleate and grow on the compression side of the nanowire (beneath the central load contact), rather than on the tensile side. This behavior reflects the stress asymmetry induced by the concentrated bending moment: although classical beam theory predicts tensile-driven slip at the bottom surface, the high localized compressive stresses under the loading contact favor dislocation nucleation on inclined {111} planes. With continued straining, stacking faults expand, interact, and coalesce, leading to the formation of a distinct plastic hinge that accommodates the imposed bending moment.

These deformation mechanisms are broadly consistent with prior studies, which have revealed that three-point bending of nanowires can activate complex deformation modes beyond simple elastic bending. Factors such as end constraints, wire dimensions, and large deflections introduce significant uncertainties in Young's modulus measurements during bending experiments [44]. In addition, in situ characterization techniques such as coherent X-ray diffraction and Laue micro-diffraction have shown that torsional deformation can accompany bending, even when purely bending loads are applied [45], [46]. These advanced methods allow quantification of bending and torsion angles and have demonstrated that plastic deformation in metallic nanowires involves the storage of GNDs and the activation of unexpected slip systems.

Adhesive forces between the nanowire and the supporting substrate can also significantly alter boundary conditions, further complicating the mechanical response and its interpretation[47]. These insights highlight the intrinsic complexity of nanowire bending mechanics and underscore the importance of careful modeling and advanced characterization when analyzing deformation at the nanoscale.

4.2 Shear Loading

Rectangular Ag nanowires, measuring 16 nm along the x direction$[\bar{1}\bar{1}0]$, 10 nm in the y direction $[11\bar{2}]$, and 29.3 nm in the z direction [111], were modeled with five periodically repeating twin boundaries oriented parallel to the x–y plane and spaced along the z direction. The simulations were conducted at a temperature of 300 K. To assess the influence of loading orientation on deformation behavior, shear loads were applied along two orthogonal directions. In the atomic visualizations, figure 4.8 and 4.9, the outermost atomic layers were removed to better reveal internal deformation structures; green atoms represent FCC lattice sites, while red atoms correspond to atoms adopting a HCP configuration.

4.2.1 Force Applied Along The $[11\bar{2}]$ Direction

When the shear load of F = 0.007 is applied along the $[11\bar{2}]$ direction, the nanowire initially responds elastically, exhibiting uniform lattice deformation without permanent structural changes. As shear strain accumulates under continued loading, the material response transitions from elastic to plastic. The earliest indication of plastic deformation is observed as a downward shift of the top twin boundary (TB1), as shown in Figures 4.8(a)-(f). This movement of the twin boundary is a characteristic manifestation of twin boundary migration, marking the onset of localized plasticity within the nanowire.

Twin boundary (TB) migration in face-centered cubic (FCC) metals occurs through the sequential nucleation and glide of twinning partial dislocations on {111} planes adjacent to the twin interface. A twin boundary separates two mirror-symmetric regions of the crystal lattice and possesses relatively low interfacial energy. Under applied shear or normal stresses, partial dislocations nucleate at the twin boundary and propagate across atomic planes, shifting the boundary by one atomic layer with each successive glide event. This process causes the twin region to either grow or shrink, depending on the direction of migration relative to the applied stress. Importantly, elastic anisotropy influences the propensity for twin boundary migration, with higher elastic anisotropy ratios enhancing twinnability under combined shear and normal loading conditions [48].

Beyond mechanical driving forces, twin boundary energy (TBE) plays a central role in twin formation and migration. Lower TBE values favor easier twin nucleation and growth, as revealed by first-principles calculations linking TBE magnitudes to the intrinsic twinning ability of different FCC metals [49]. In addition, twin boundaries can serve as efficient sinks for point defects such as self-interstitials, with the aggregation of self-interstitial clusters within twin planes further modifying local boundary mobility and stress distributions [50].

TB-dislocation interactions also significantly impact the migration and mechanical behavior of twin boundaries. Interactions between lattice dislocations and twin boundaries can lead to the formation of atomic-scale steps along the boundary, dislocation pile-ups at twin lamellae ends, and even transformations into asymmetric tilt grain boundaries, all of which can either assist or hinder TB migration depending on local stress states and defect configurations [51]. Unlike conventional slip involving widespread dislocation motion, twin boundary migration enables highly localized, coordinated atomic rearrangements, allowing the material to accommodate significant shear strains while preserving crystallographic order [52]. Migration of twin boundaries can be thermally activated or stress-driven, particularly at the nanoscale where stress concentrations are high. This deformation mode plays a critical role in enhancing the strength, ductility, and strain hardening behavior of nanostructured metals.

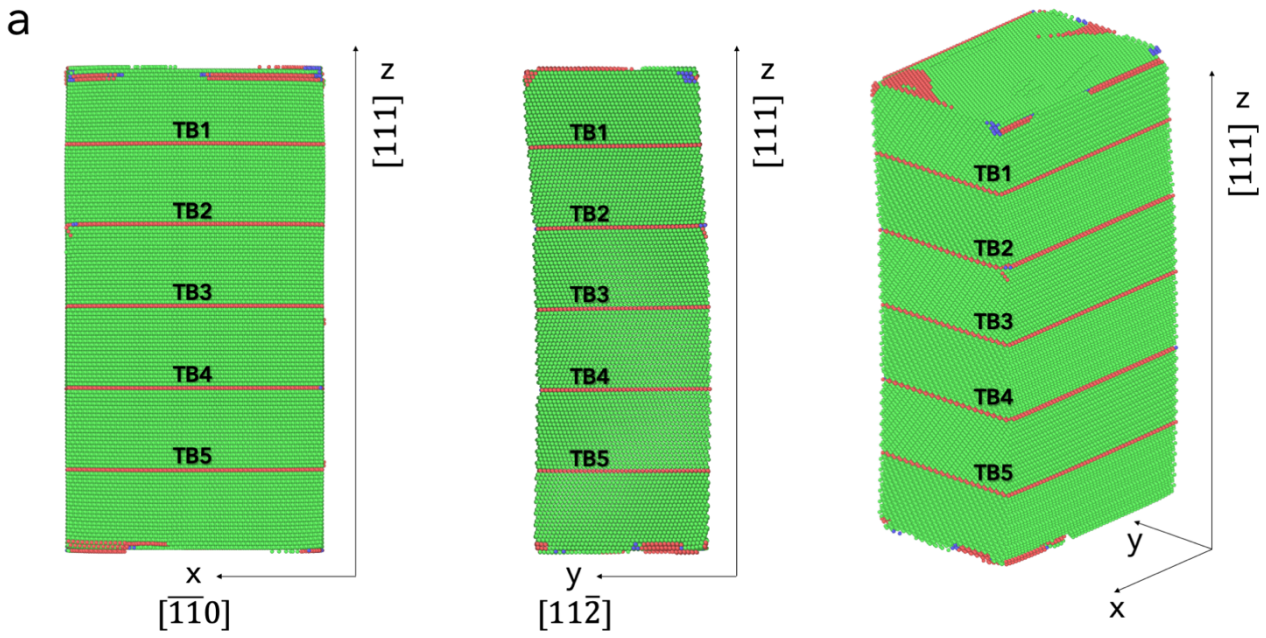

Figure 4.8: ABC snapshots of shear loading applied along the $[11\bar{2}]$ direction. Multi-perspective illustration of the nanowire undergoing shear deformation, viewed from three different angles. The outermost atomic layers have been removed to better reveal internal deformation structures. Green atoms represent FCC environments, and red atoms indicate HCP stacking faults.

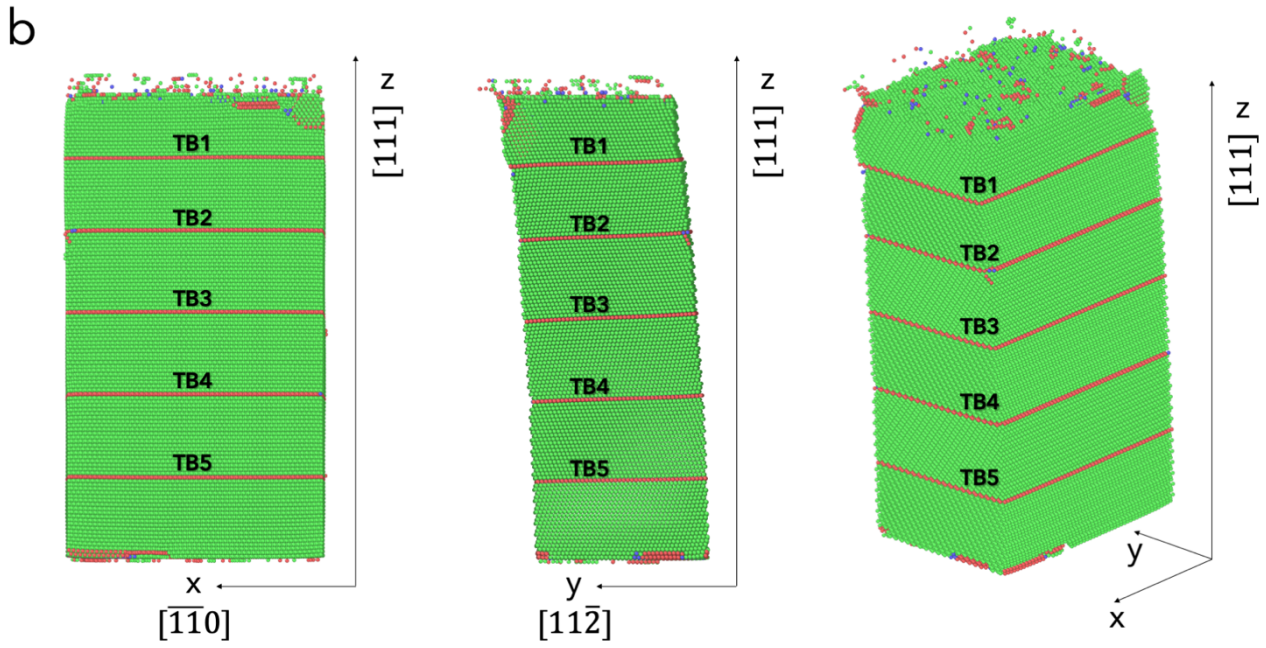

Figure 4.8 (b), early-stage deformation under constant applied force. The nanowire exhibits uniform elastic deformation, with pre-existing twin boundaries remaining clearly visible and unchanged in position.

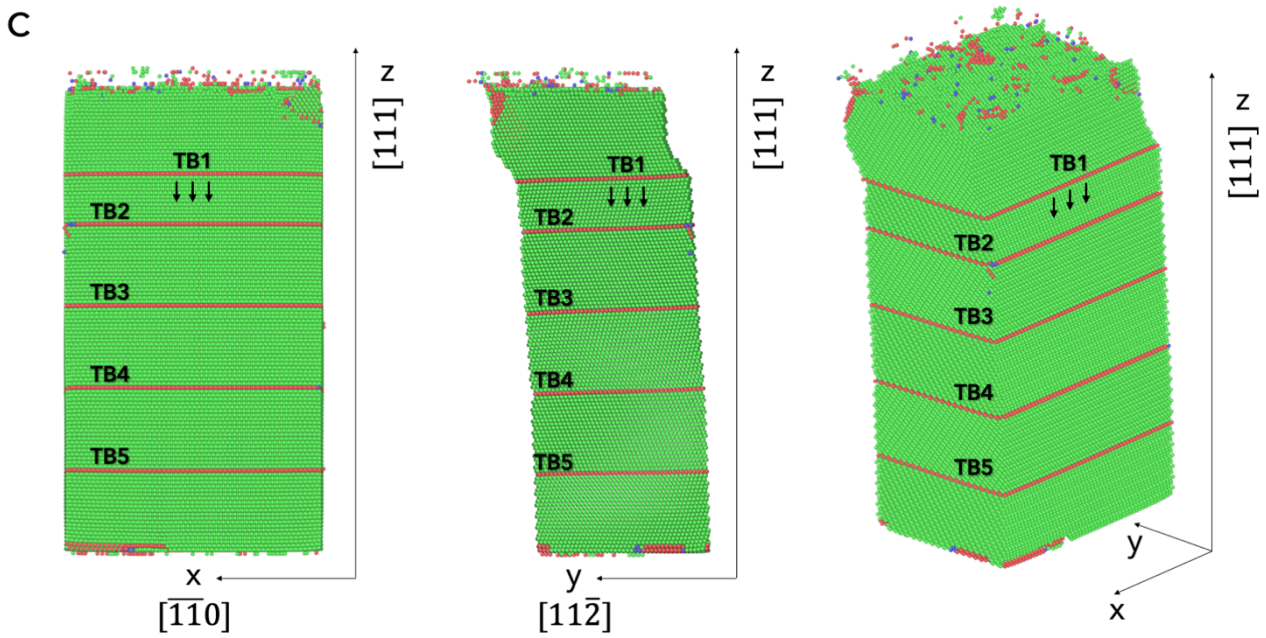

Figure 4.8 (c) onset of plasticity characterized by the initial migration of the top twin boundary (TB1). The downward shift of TB1 marks the beginning of twin boundary migration under persistent shear loading.

As shear strain continues to accumulate, additional planar defects develop. Dislocation nucleation predominantly occurs at free-surface corners, where stress concentrations are highest, rapidly leading to stacking fault formation. These

stacking faults appear as distinct two-layer red-atom regions aligned parallel to the x-y plane. The observations highlight the interplay between twin boundary migration, stacking fault formation, and localized plasticity within the nanowire.

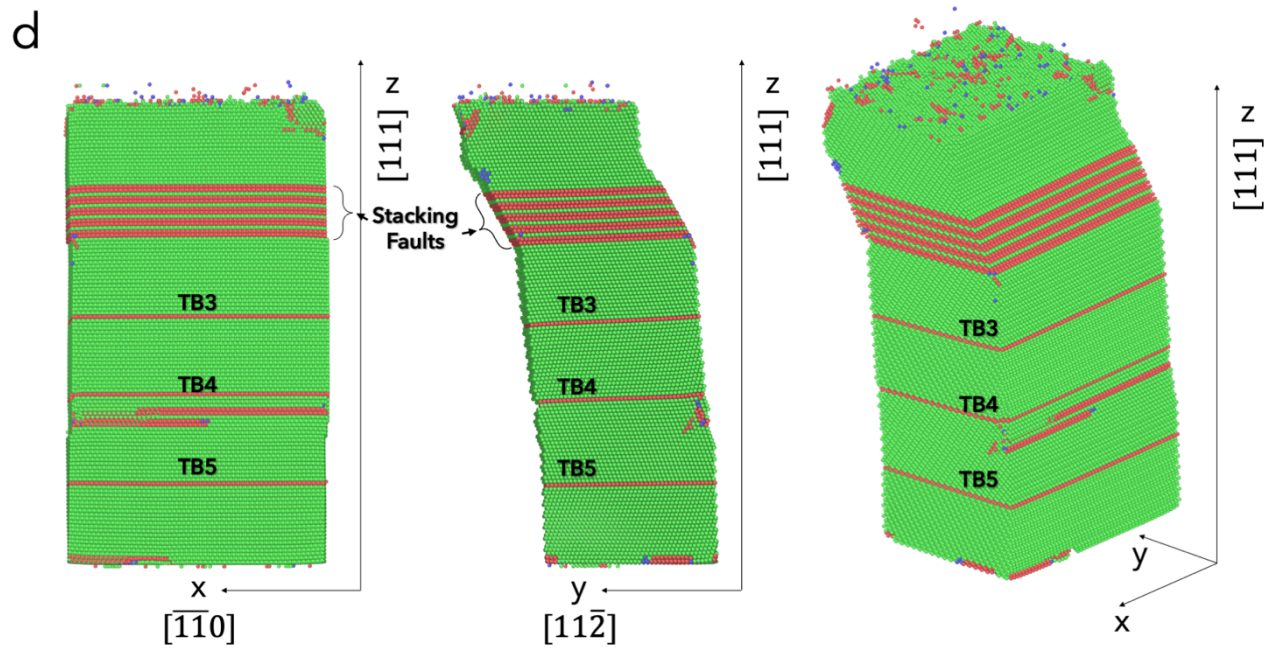

Figure 4.8 (d) emergence of additional stacking faults as deformation progresses. Distinct two-layer HCP regions appear, aligned parallel to the x–y plane, consistent with partial dislocation glide on {111} planes and continued plastic deformation.

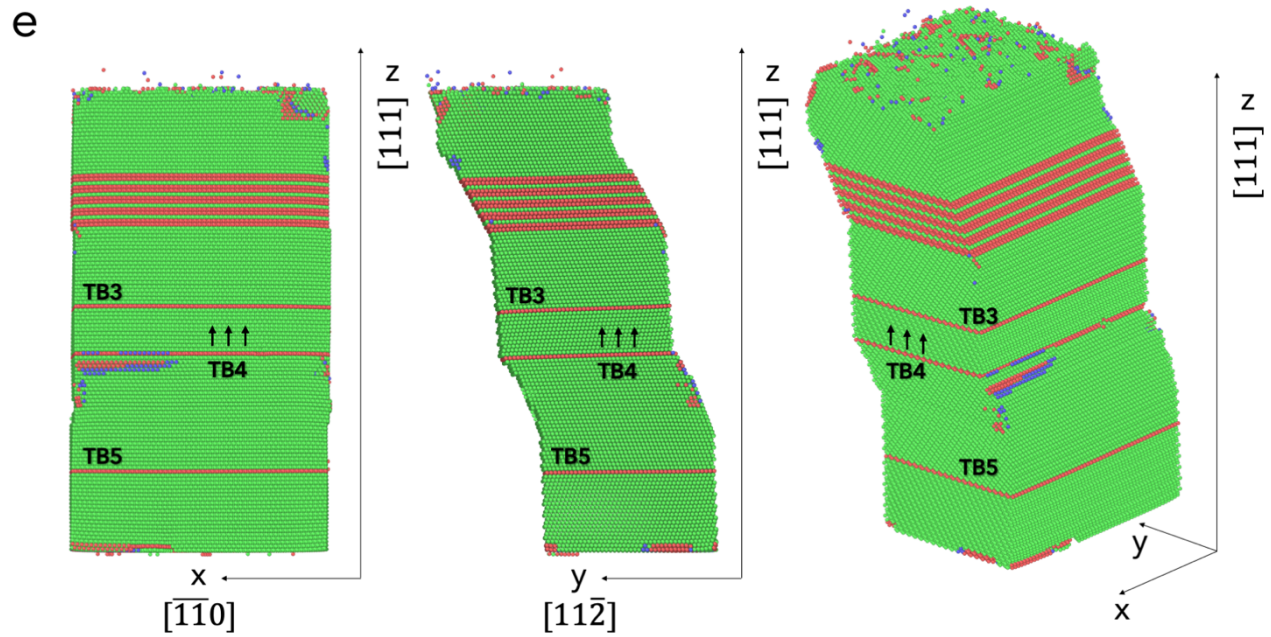

Figure 4.8 (e) continued deformation revealing non-uniform twin boundary migration. TB4 begins to migrate upward, indicating differential twin boundary responses within the nanowire under shear loading.

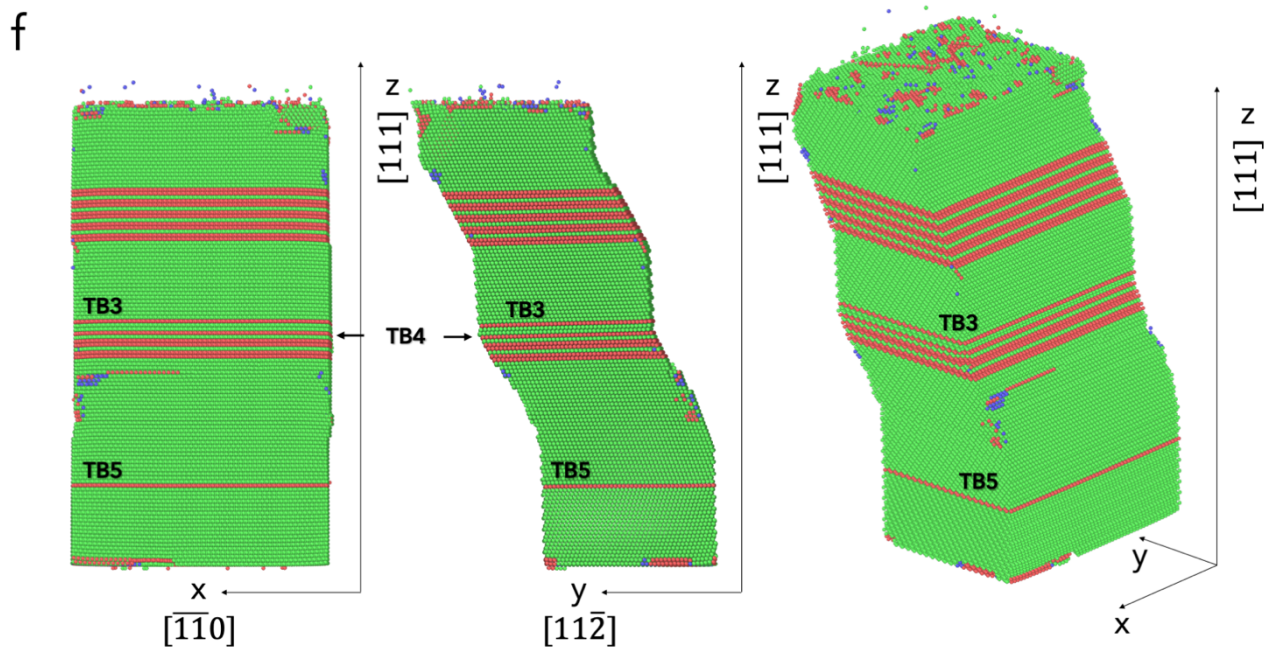

Figure 4.8 (f) Final deformed state of the nanowire. Prominent stacking faults persist near the top, while twin boundaries TB3, TB4, and TB5 are retained in the middle and lower sections of the nanowire, evidencing complex localized plastic accommodation.

4.2.2 Force Applied Along The [$\bar{1}\bar{1}$0] Direction

In contrast, when the same magnitude of force is applied along the [$\bar{1}\bar{1}$0] direction, the nanowire exhibits a markedly different deformation behavior. From the very onset of loading, the wire undergoes immediate plastic deformation with no observable elastic phase. Instead of twin boundary migration as the initial plastic event, dislocations rapidly nucleate at the free-surface corners and form stacking faults. As shear strain increases, these stacking faults, which are again evident as distinct two-layer red-atom regions parallel to the x–y plane, dominate the deformation process. Importantly, under X-direction loading, none of the stacking faults transition into new twin boundaries, and no twin boundary migration is observed.

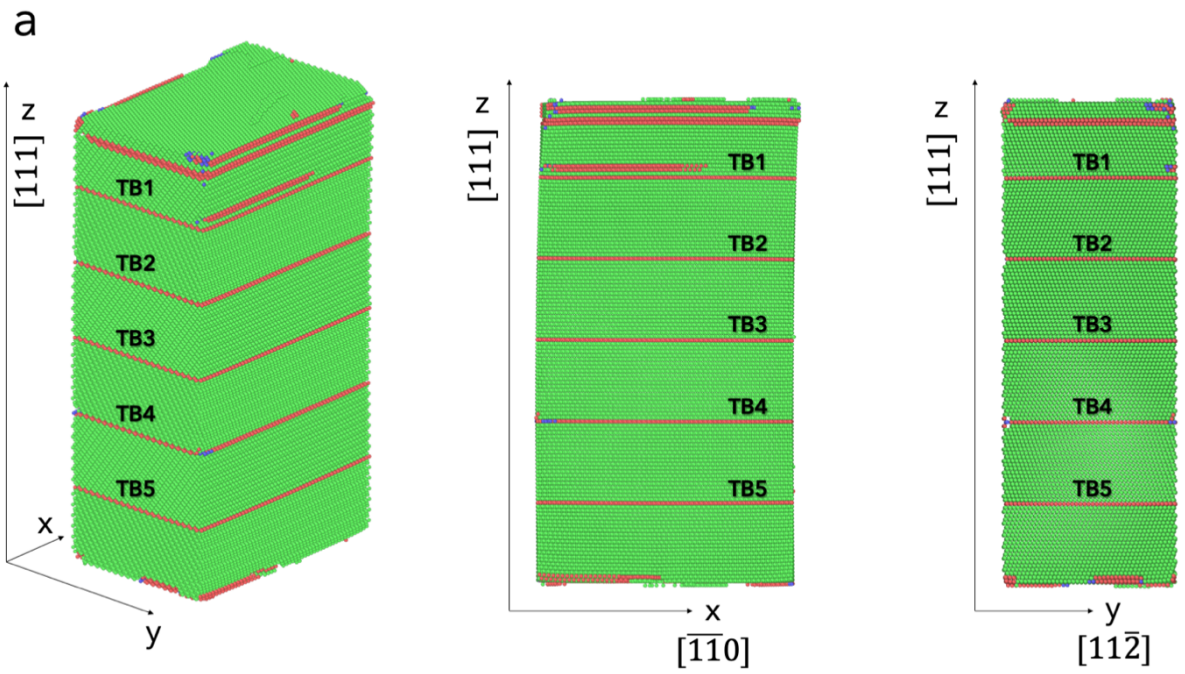

Figure 4.9 (a), nanowire undergoing shear loading applied along the $[\bar{1}\bar{1}0]$ direction, this image shows the onset of plasticity as soon as the shear load is applied in the x direction. Dislocation nucleation is visible at the free surfaces, and initial stacking faults begin to form.

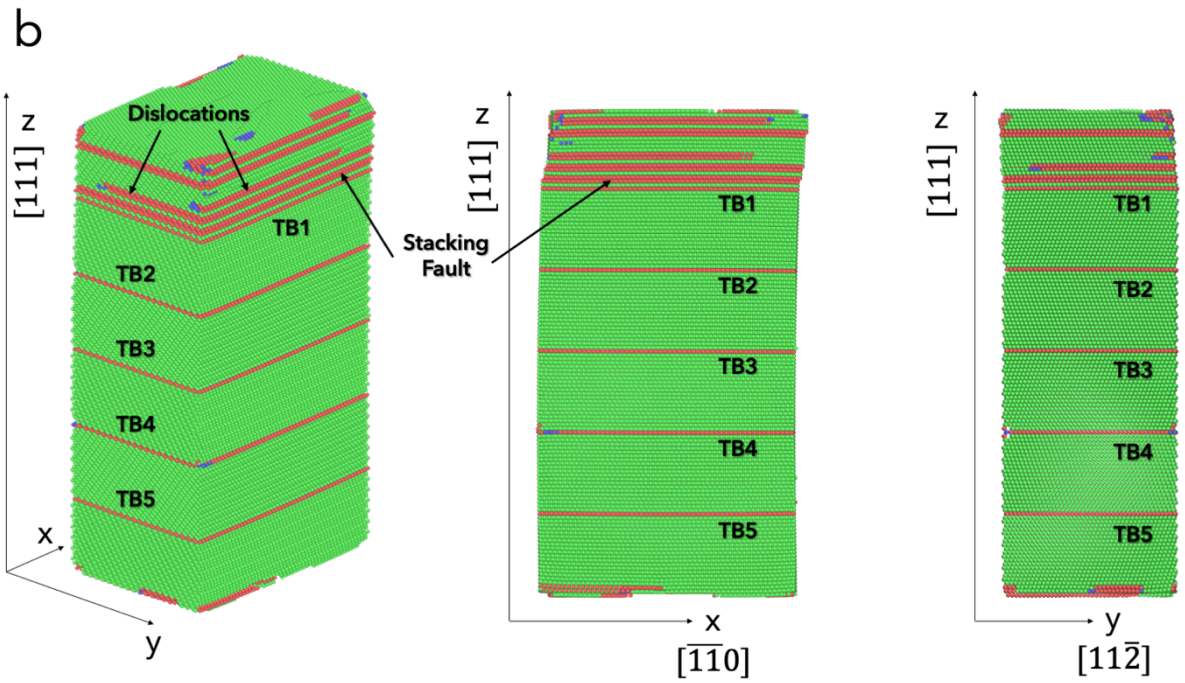

Figure 4.9 (b), stacking faults become more pronounced and are clearly visible. The faults develop rapidly from the early nucleated dislocations, indicating an immediate plastic response under x-direction loading.

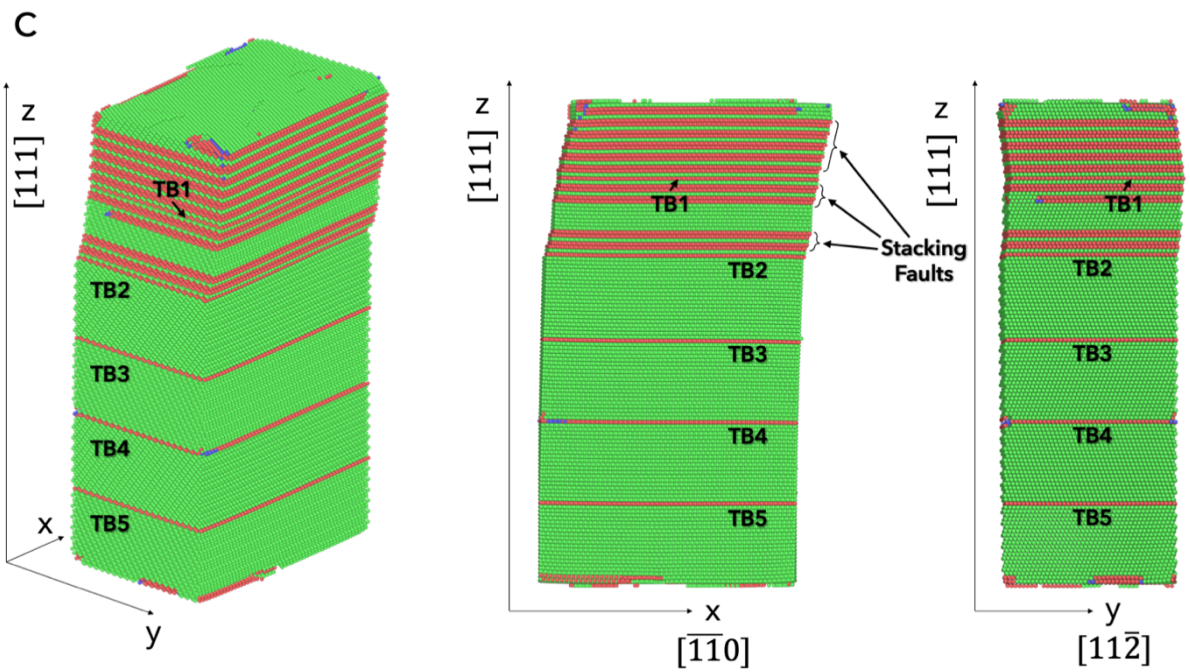

Figure 4.9 (c), as the number of stacking faults increases, the nanowire displays a straight slope when viewed in the xz plane. This suggests that the accumulation of stacking faults is stabilizing the deformation in this plane, even as plastic activity continues.

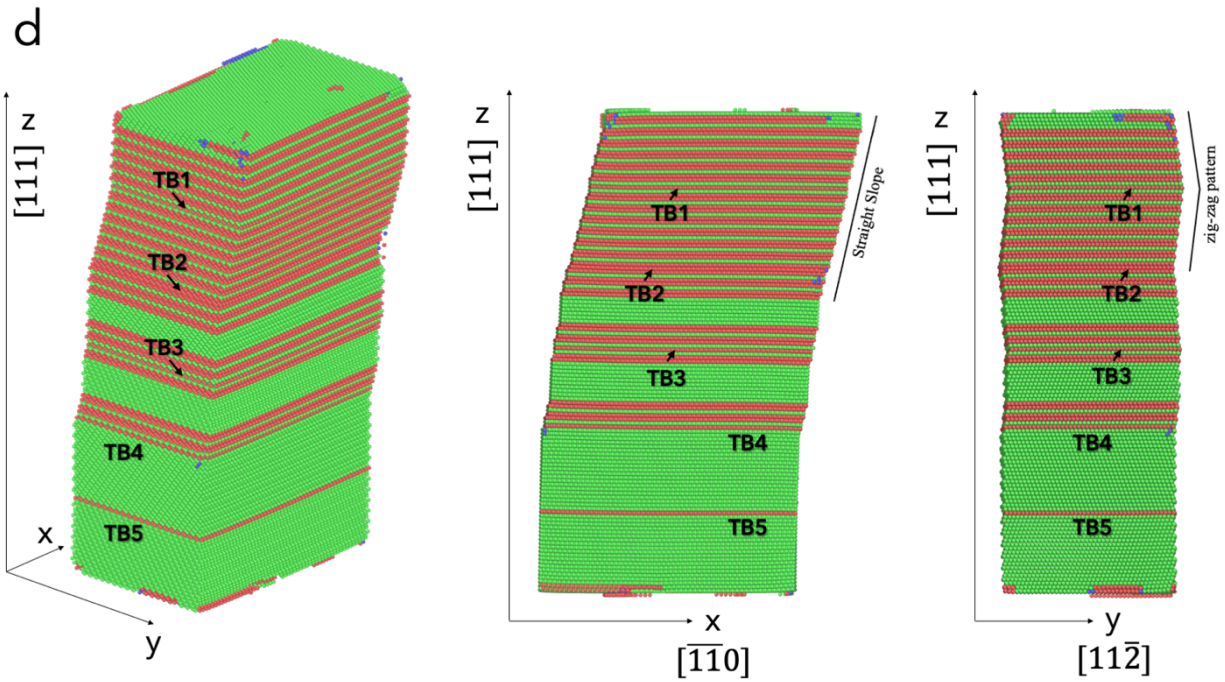

Figure 4.9 (d), With further strain, the nanowire begins to develop a straight slope in the xz plane, and a distinct zig-zag pattern when viewed in the yz plane. This pattern reflects the heterogeneous distribution of stacking faults across the cross-section and indicates complex dislocation interactions under the applied x-direction shear load.

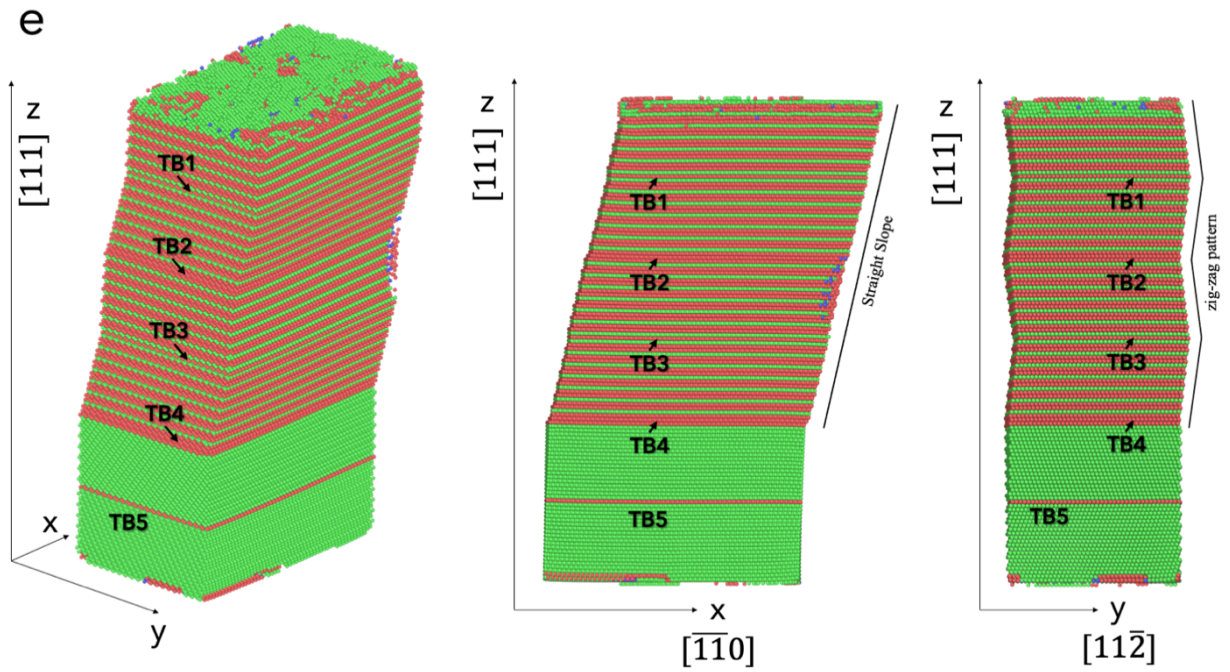

Figure 4.9 (e): In the final configuration, the xz view reveals a consistent, straight slope, while the yz plane view displays a pronounced zig-zag pattern. Throughout the deformation process, stacking faults proliferate extensively without any twin boundary migration, emphasizing that the plastic response under x-direction loading is dominated by dislocation nucleation and stacking fault formation.

These results clearly demonstrate that simply changing the loading direction, from $[11\bar{2}]$ to $[\bar{1}\bar{1}0]$, while using the same nanowire model and simulation setup, produces fundamentally different deformation mechanisms. Under $[11\bar{2}]$ direction loading, plasticity is accommodated primarily by twin boundary migration, whereas under $[\bar{1}\bar{1}0]$ direction loading, deformation is characterized by immediate dislocation nucleation and stacking fault formation without significant twin activity. Despite the severe localized plasticity observed in both cases, the overall structural geometry of the nanowire is preserved after yielding, illustrating the strong directional dependence of deformation behavior in nanoscale silver wires.

These findings highlight the critical role of crystallographic orientation and loading direction in dictating the dominant plasticity mechanisms at the nanoscale. Understanding this sensitivity is essential for the design and application of nanostructured materials, where mechanical performance, defect evolution, and structural stability can be tailored through control of twin boundary configurations and loading geometry. The results further emphasize that nanoscale deformation cannot be assumed to be isotropic, and careful consideration of orientation effects is necessary for the reliable integration of metallic nanowires into functional applications.

CHAPTER FIVE: CONCLUSIONS AND FUTURE WORK

This thesis presents an in-depth investigation into deformation mechanisms in metallic nanowires subjected to bending and shear stresses using advanced computational modeling approaches. The primary objective was to overcome the inherent timescale limitations of MD simulations through the implementation of the ABC method. Key finding of this research include:

- ABC simulations demonstrated their capability to mitigate the timescale limitations associated with MD, offering valuable insights into slow and time-dependent deformation processes in nanowire systems, particularly effective for systems comprising fewer than 10,000 atoms.

- Nanowire deformation behaviors are significantly influenced by size, crystallographic orientation, and loading conditions, with primary mechanisms identified as dislocation nucleation and propagation, twinning and detwinning, twin-boundary migration, and the formation of FFT boundaries.

- Comparative analyses of MD and ABC simulations highlight pronounced directional dependence of deformation mechanisms in silver and gold nanowires. Under bending and shear conditions, deformation behaviors notably differ according to the applied load direction. Specifically, MD simulations in top-bending tests of silver nanowires identified loading conditions below the yield point, thus primarily capturing elastic deformation due to their inherent short-timescale constraints. In contrast, ABC simulations effectively detected significant plastic deformation, mimicking long-term creep behaviors, characterized by the nucleation of stacking faults and twin-boundary migration.

- Both MD and ABC simulations revealed the formation of FFT boundaries under increased loading conditions. MD simulations indicated rapid FFT formation above a critical stress, resulting in the immediate emergence of multiple FFT structures. ABC simulations, however, exhibited gradual FFT formation, aligning with its capability to mimic slow, long-term deformation processes. Once formed, these FFT structures persist, leaving the nanowire permanently bent and plastically deformed.

- Distinct responses were observed in gold nanowires under shear loading in different crystallographic orientations. Loading in the Y-direction promoted twin-boundary migration and defect evolution, while loading in the X-direction primarily resulted in rapid dislocation nucleation and persistent stacking fault formation, absent of twin-boundary activities.

Several limitations identified within this study provide potential directions for future research:

- ABC simulations remain computationally demanding, limiting their current applicability primarily to smaller-scale atomic systems. Enhancing computational efficiency and scalability remains a priority for broader implementation.

- The accuracy and effectiveness of ABC simulations are highly sensitive to parameter selection. Therefore, future developments should aim at creating automated and adaptive parameter optimization frameworks. Such automation could dynamically adjust parameters based on ongoing simulation outcomes, significantly improving both the practical usability and the reliability of ABC simulations.

- Real-world experimental validation of ABC simulation results is critically important, yet challenging due to limited experimental data at the atomic scale. Expanding experimental investigations to produce extensive, detailed datasets is crucial for rigorous validation and enhancement of computational models.

In conclusion, this research contributes to an improved understanding of deformation mechanisms in metallic nanowires. The effectiveness demonstrated by ABC simulations highlights their potential as a complementary approach to traditional MD simulations, particularly in investigating deformation phenomena occurring over extended timescales. These advancements enhance computational capabilities, offering a strong foundation for future research aimed at optimizing the performance and reliability of nanoscale materials.

REFERENCES

[1] Md. S. Oliullah et al., “A Comprehensive Review on the Advances of Nanowires in Multidisciplinary Applications,” Nano LIFE, vol. 14, no. 04, p. 2440005, Dec. 2024, doi: 10.1142/S1793984424400051.

[2] N. I. Goktas, P. Wilson, A. Ghukasyan, D. Wagner, S. McNamee, and R. R. LaPierre, “Nanowires for energy: A review,” Appl. Phys. Rev., vol. 5, no. 4, p. 041305, Dec. 2018, doi: 10.1063/1.5054842.

[3] S. Wang, Z. Shan, and H. Huang, “The Mechanical Properties of Nanowires,” Adv. Sci., vol. 4, no. 4, p. 1600332, Apr. 2017, doi: 10.1002/advs.201600332.

[4] Y. Cui, Q. Wei, H. Park, and C. M. Lieber, “Nanowire Nanosensors for Highly Sensitive and Selective Detection of Biological and Chemical Species,” Science, vol. 293, no. 5533, pp. 1289–1292, Aug. 2001, doi: 10.1126/science.1062711.

[5] X. Wang et al., “Atomistic processes of surface-diffusion-induced abnormal softening in nanoscale metallic crystals,” Nat. Commun., vol. 12, no. 1, p. 5237, Sep. 2021, doi: 10.1038/s41467-021-25542-2.

[6] H. G. Craighead, “Nanoelectromechanical Systems,” Science, vol. 290, no. 5496, pp. 1532–1535, Nov. 2000, doi: 10.1126/science.290.5496.1532.

[7] Y. Xia et al., “One-Dimensional Nanostructures: Synthesis, Characterization, and Applications,” Adv. Mater., vol. 15, no. 5, pp. 353–389, Mar. 2003, doi: 10.1002/adma.200390087.

[8] Z. L. Wang and J. Song, “Piezoelectric Nanogenerators Based on Zinc Oxide Nanowire Arrays,” Science, vol. 312, no. 5771, pp. 242–246, Apr. 2006, doi: 10.1126/science.1124005.

[9] L. Hu, H. S. Kim, J.-Y. Lee, P. Peumans, and Y. Cui, “Scalable Coating and Properties of Transparent, Flexible, Silver Nanowire Electrodes,” ACS Nano, vol. 4, no. 5, pp. 2955–2963, May 2010, doi: 10.1021/nn1005232.

[10] J. Sort, “Nanocomposite Materials: A Section of Nanomaterials,” Nanomaterials, vol. 12, no. 2, p. 203, Jan. 2022, doi: 10.3390/nano12020203.

[11] C. Jia, Z. Lin, Y. Huang, and X. Duan, “Nanowire Electronics: From Nanoscale to Macroscale,” Chem. Rev., vol. 119, no. 15, pp. 9074–9135, Aug. 2019, doi: 10.1021/acs.chemrev.9b00164.

[12] A. H. Chokshi, “Grain Boundary Processes in Strengthening, Weakening, and Superplasticity,” Adv. Eng. Mater., vol. 22, no. 1, p. 1900748, Jan. 2020, doi: 10.1002/adem.201900748.

[13] C. Deng, “Characterization of Nanomaterials: Computational Modeling,” presented at the ME 4350 Properties and Applications of Nanomaterials, University of Manitoba, Fall 2024.

[14] G. Fraux, S. Chibani, and F.-X. Coudert, “Modelling of framework materials at multiple scales: current practices and open questions,” Philos. Trans. R. Soc. Math. Phys. Eng. Sci., vol. 377, no. 2149, p. 20180220, Jul. 2019, doi: 10.1098/rsta.2018.0220.

[15] “Practical considerations for Molecular Dynamics,” GitHub. [Online]. Available: https://computecanada.github.io/molmodsim-md-theory-lesson-novice/

[16] X. Yan, P. Cao, W. Tao, P. Sharma, and H. S. Park, “Atomistic modeling at experimental strain rates and timescales,” J. Phys. Appl. Phys., vol. 49, no. 49, p. 493002, Dec. 2016, doi: 10.1088/0022-3727/49/49/493002.

[17] P. Tiwary and A. Van De Walle, “A Review of Enhanced Sampling Approaches for Accelerated Molecular Dynamics,” in Multiscale Materials Modeling for Nanomechanics, vol. 245, C. R. Weinberger and G. J. Tucker, Eds., in Springer Series in Materials Science, vol. 245. , Cham: Springer International Publishing, 2016, pp. 195–221. doi: 10.1007/978-3-319-33480-6_6.

[18] S. Yefimov, E. V. D. Giessen, and I. Groma, “Bending of a single crystal: discrete dislocation and nonlocal crystal plasticity simulations,” Model. Simul. Mater. Sci. Eng., vol. 12, no. 6, pp. 1069–1086, Nov. 2004, doi: 10.1088/0965-0393/12/6/002.

[19] S. Sandfeld, T. Hochrainer, P. Gumbsch, and M. Zaiser, “Numerical implementation of a 3D continuum theory of dislocation dynamics and application to micro-bending,” Philos. Mag., vol. 90, no. 27–28, pp. 3697–3728, Sep. 2010, doi: 10.1080/14786430903236073.

[20] F. Weber, I. Schestakow, F. Roters, and D. Raabe, “Texture Evolution During Bending of a Single Crystal Copper Nanowire Studied by EBSD and Crystal Plasticity Finite Element Simulations,” Adv. Eng. Mater., vol. 10, no. 8, pp. 737–741, Aug. 2008, doi: 10.1002/adem.200800102.

[21] J. He and C. M. Lilley, “Surface Effect on the Elastic Behavior of Static Bending Nanowires,” Nano Lett., vol. 8, no. 7, pp. 1798–1802, Jul. 2008, doi: 10.1021/nl0733233.

[22] Y. Zhu et al., “Size effects on elasticity, yielding, and fracture of silver nanowires: In situ experiments,” Phys. Rev. B, vol. 85, no. 4, p. 045443, Jan. 2012, doi: 10.1103/PhysRevB.85.045443.

[23] K. Kolluri, M. R. Gungor, and D. Maroudas, “Molecular-dynamics simulations of stacking-fault-induced dislocation annihilation in prestrained ultrathin single-crystalline copper films,” J. Appl. Phys., vol. 105, no. 9, p. 093515, May 2009, doi: 10.1063/1.3120916.

[24] A. J. Cao, Y. G. Wei, and S. X. Mao, “Deformation mechanisms of face-centered-cubic metal nanowires with twin boundaries,” Appl. Phys. Lett., vol. 90, no. 15, p. 151909, Apr. 2007, doi: 10.1063/1.2721367.

[25] S.-H. Kim, J.-H. Park, H.-K. Kim, J.-P. Ahn, D.-M. Whang, and J.-C. Lee, “Twin boundary sliding in single crystalline Cu and Al nanowires,” Acta Mater., vol. 196, pp. 69–77, Sep. 2020, doi: 10.1016/j.actamat.2020.06.028.

[26] Q. Zhu et al., “Revealing extreme twin-boundary shear deformability in metallic nanocrystals,” Sci. Adv., vol. 7, no. 36, p. eabe4758, Sep. 2021, doi: 10.1126/sciadv.abe4758.

[27] H. S. Park, K. Gall, and J. A. Zimmerman, “Deformation of FCC nanowires by twinning and slip,” J. Mech. Phys. Solids, vol. 54, no. 9, pp. 1862–1881, Sep. 2006, doi: 10.1016/j.jmps.2006.03.006.

[28] Z. Ren et al., “Three-point bending behavior of a Au nanowire studied by in-situ Laue micro-diffraction,” J. Appl. Phys., vol. 124, no. 18, p. 185104, Nov. 2018, doi: 10.1063/1.5054068.

[29] C. R. Weinberger and W. Cai, “Plasticity of metal nanowires,” J. Mater. Chem., vol. 22, no. 8, p. 3277, 2012, doi: 10.1039/c2jm13682a.

[30] X. Wang, S. Zheng, C. Deng, C. R. Weinberger, G. Wang, and S. X. Mao, “In Situ Atomic-Scale Observation of 5-Fold Twin Formation in Nanoscale Crystal under Mechanical Loading,” Nano Lett., vol. 23, no. 2, pp. 514–522, Jan. 2023, doi: 10.1021/acs.nanolett.2c03852.

[31] Y. Chen, Q. Huang, S. Zhao, H. Zhou, and J. Wang, “Interactions between Dislocations and Penta-Twins in Metallic Nanocrystals,” Metals, vol. 11, no. 11, p. 1775, Nov. 2021, doi: 10.3390/met11111775.

[32] Y. Chen, Q. Huang, S. Zhao, H. Zhou, and J. Wang, “Penta-Twin Destruction by Coordinated Twin Boundary Deformation,” Nano Lett., vol. 21, no. 19, pp. 8378–8384, Oct. 2021, doi: 10.1021/acs.nanolett.1c02970.

[33] X. Wang, S. Zheng, C. Deng, C. R. Weinberger, G. Wang, and S. X. Mao, “In Situ Atomic-Scale Observation of 5-Fold Twin Formation in Nanoscale Crystal under Mechanical Loading,” Nano Lett., vol. 23, no. 2, pp. 514–522, Jan. 2023, doi: 10.1021/acs.nanolett.2c03852.

[34] “LAMMPS Documentation (2 Apr 2025 version),” LAMMPS. [Online]. Available: https://docs.lammps.org/Manual.html

[35] S. Jin et al., “On the temperature dependence of the density of states of liquids at low energies,” Sci. Rep., vol. 14, no. 1, p. 18805, Aug. 2024, doi: 10.1038/s41598-024-69504-2.

[36] P. Cao, M. Li, R. J. Heugle, H. S. Park, and X. Lin, “Self-learning metabasin escape algorithm for supercooled liquids,” Phys. Rev. E, vol. 86, no. 1, p. 016710, Jul. 2012, doi: 10.1103/PhysRevE.86.016710.

[37] P. Cao, M. P. Short, and S. Yip, “Potential energy landscape activations governing plastic flows in glass rheology,” Proc. Natl. Acad. Sci., vol. 116, no. 38, pp. 18790–18797, Sep. 2019, doi: 10.1073/pnas.1907317116.

[38] B. Roos, B. Kapelle, G. Richter, and C. A. Volkert, “Surface dislocation nucleation controlled deformation of Au nanowires,” Appl. Phys. Lett., vol. 105, no. 20, p. 201908, Nov. 2014, doi: 10.1063/1.4902313.

[39] S. Sarkar, “Extending the Time Scale in Atomistic Simulations: The Diffusive Molecular Dynamics Method,” Doctor of Philosophy, Ohio State University, 2011. [Online]. Available: http://rave.ohiolink.edu/etdc/view?acc_num=osu1321282489

[40] Y. Tao, Y. Zhao, Z. Wang, L. Fu, and L. Wang, “Deformation Mechanisms of FCC-Structured Metallic Nanocrystal with Incoherent Twin Boundary,” Metals, vol. 11, no. 11, p. 1672, Oct. 2021, doi: 10.3390/met11111672.

[41] Y. G. Zheng, H. W. Zhang, Z. Chen, L. Wang, Z. Q. Zhang, and J. B. Wang, “Formation of two conjoint fivefold deformation twins in copper nanowires with molecular dynamics simulation,” Appl. Phys. Lett., vol. 92, no. 4, p. 041913, Jan. 2008, doi: 10.1063/1.2839581.

[42] Y. Yue, Q. Zhang, Z. Yang, Q. Gong, and L. Guo, “Study of the Mechanical Behavior of Radially Grown Fivefold Twinned Nanowires on the Atomic Scale,” Small, vol. 12, no. 26, pp. 3503–3509, Jul. 2016, doi: 10.1002/smll.201600038.

[43] J. Y. Wu, S. Nagao, J. Y. He, and Z. L. Zhang, “Role of Five-fold Twin Boundary on the Enhanced Mechanical Properties of fcc Fe Nanowires,” Nano Lett., vol. 11, no. 12, pp. 5264–5273, Dec. 2011, doi: 10.1021/nl202714n.

[44] P. Zhou, C. Wu, and X. Li, “Three-point bending Young’s modulus of nanowires,” Meas. Sci. Technol., vol. 19, no. 11, p. 115703, Nov. 2008, doi: 10.1088/0957-0233/19/11/115703.

[45] A. Davydok et al., “In Situ Coherent X-ray Diffraction during Three-Point Bending of a Au Nanowire: Visualization and Quantification,” Quantum Beam Sci., vol. 2, no. 4, p. 24, Nov. 2018, doi: 10.3390/qubs2040024.

[46] Z. Ren et al., “Three-point bending behavior of a Au nanowire studied by in-situ Laue micro-diffraction,” J. Appl. Phys., vol. 124, no. 18, p. 185104, Nov. 2018, doi: 10.1063/1.5054068.

[47] Y. Zhang and Y.-P. Zhao, “Adhesive Contact of Nanowire in Three-Point Bending Test,” J. Adhes. Sci. Technol., vol. 25, no. 10, pp. 1107–1129, Jan. 2011, doi: 10.1163/016942410X549898.

[48] H. Xie et al., “Driving force of zero-macroscopic-strain deformation twinning in face-centred-cubic metals,” Philos. Mag., vol. 101, no. 21, pp. 2318–2330, Nov. 2021, doi: 10.1080/14786435.2021.1971317.

[49] L. Liu et al., “First-principles calculations of twin-boundary energies in face-centered-cubic metals,” Int. J. Mod. Phys. B, vol. 38, no. 23, p. 2450312, Sep. 2024, doi: 10.1142/S0217979224503120.

[50] M. I. Mendelev and A. H. King, “The interactions of self-interstitials with twin boundaries,” Philos. Mag., vol. 93, no. 10–12, pp. 1268–1278, Apr. 2013, doi: 10.1080/14786435.2012.747012.

[51] X. Gao, L. Dai, and Y. Zhao, “Twin boundary-dislocation interactions in nanocrystalline Cu-30% Zn alloys prepared by high pressure torsion,” J. Mater. Res. Technol., vol. 9, no. 5, pp. 11958–11967, Sep. 2020, doi: 10.1016/j.jmrt.2020.08.060.

[52] T. Kizuka, “Atomistic Process of Twin-Boundary Migration Induced by Shear Deformation in Gold,” Jpn. J. Appl. Phys., vol. 46, no. 11R, p. 7396, Nov. 2007, doi: 10.1143/JJAP.46.7396.